CyclObs Database

TC Vortex Analysis Product

Léo Vinour (IFREMER)
Théo Cévaer (OceanScope)
Alexis Mouche (IFREMER)
Olivier Archer (IFREMER)

CyclObs Database
TC Vortex Analysis Product

by

Léo Vinour (IFREMER)
Théo Cévaer (OceanScope)
Alexis Mouche (IFREMER)
Olivier Archer (IFREMER)

Document version	1.0
Institution:	Institut Français de Recherche pour l'Exploitation de la MER
Document Date:	Monday 19th September, 2022

Contents

1 Introduction

1.1. Purpose

This document describes the C-Band SAR Tropical Cyclone Vortex Analysis (TCVA) Products.

1.2. Product objective

The TCVA product family aims at providing an independent characterization of TC vortex at high resolution from SAR data.

In particular, it includes an estimate of the following TC parameters :

- storm center
- radius of maximum wind speed
- eye shape
- wind radii

TCVA product also allows to define TC parameters (such as the wind radii) usually defined in a geographical referential (especially for marine safety purposes) in the referential of the considered storm for new applications.

Finally TCVA product is also a gridded product containing the wind field in the two aforementioned referential and with different systems of coordinates (cartesian and polar).

1.3. Product motivations

While a variety of sources for Tropical Cyclone (TC) wind data is now available (e.g. (Reul et al., 2017), the only routine high resolution observations comes from aircraft reconnaissance flights, limited to TCs occuring in the North Atlantic and East Pacific. In this context, C-Band high resolution radar (or SAR for Synthetic Aperture Radar) is the only space-borne instrument able to probe and uniquely quantify, at very high spatial resolution O(1 km), ocean sea surface information under extreme conditions (Katsaros et al., 2000; Horstmann et al., 2013; Zhang and Perrie, 2012; Horstmann et al., 2015). Indeed, SAR can provide measurements at day and night, regardless the cloud coverage, with a pixel resolution of few meters and swaths of several hundred kilometers. For extreme weather events, such as tropical cyclones (TCs), the high-sensitivity of cross-polarized signals to ocean wave breaking has been further translated into a new potential: the use of these new cross-polarized signals to map, at very high resolution, variations in ocean surface winds in and around the TC eyes (Zhang and Perrie, 2012; Mouche et al., 2017, 2019). To date and although SAR data are routinely processed over TC, there is no available and qualified SAR database including analysis to provide TC SAR-derived parameters describing the TC vortex in the inner and outer cores. Such a product is expected to foster scientific applications.

1.4. Document structure

This document is structured as follows:

- Sentinel-1 mission and Level-2 products
- General overview of the product and processing chain
- Algorithm theoretical basis and functional description
- Product description
- User manual

2

SAR missions and Level-2 CyclObs product

2.1. General context

The TCVA product relies on C-band Radarsat-2 and Sentinel-1 Synthetic Aperture Radar (SAR) missions. C-band SAR systems operate day and night and enable to provide measurements regardless of the weather.

The MDA/CSA Radarsat-2 mission has one C-band SAR on a polar-orbiting satellite. Radarsat-2 SAR was launched in 2007 and is still operating. This is the first SAR able to provide dual- (and quad-) polarized images (VV+VH or HH+HV) with different acquisition modes including different resolutions and swath dimensions. It provides continuity with previous Canadian Radarsat-1 mission.

Sentinel-1 mission is part of the European and operational Copernicus program space component. This is a constellation of two satellites (S-1A and S-1B units). Both Sentinel-1A and -1B carry a C-band Synthetic Aperture Radar (SAR) and are also able to acquire dual-polarized images (VV+VH or HH+HV) with different acquisition modes. Sentinel-1 provides continuity with previous European ERS-1, ERS-2, and ENVISAT missions. Sentinel-1A & -1B were launched in April 2014 and 2016 respectively. Sentinel-1B is now off since the 23rd of December 2021.

Thus these two missions have the potential to acquire data over Tropical Cyclone in dual-polarization with large swath modes to capture the imprint of the TC vortex on the sea surface at synoptic scale and high resolution (<100m).

2.2. Acquisition mode and acquisition strategy

2.2.1. Acquisition modes

The TCVA product only relies on SAR acquisitions in wide swath modes chosen to maximize the TC coverage.

Sentinel-1A & -1B have four exclusive imaging modes: Interferometric Wide swath (IW), Extra Wide (EW) swath, Strip Map (SM) and Wave (WV) modes. As input data from Sentinel-1 mission, TCVA processing unit solely uses acquisitions IW and EW wide swath modes. The IW swath is 250 km wide and covers incidence angles from about 30 to 46 degrees. When processed into Level-1 (L1) GRDH (Ground Range Detected High resolution), IW Sentinel-1 products have a resolution of about 20 m in range (across-track) and 22 m in azimuth (along-track). The EW swath is 400-km wide and covers incidence angles from about 17 to 45 degrees. When processed into Level-1 (L1) GRDM (Ground Range Detected Medium resolution), EW Sentinel-1 products have a resolution of about 93 m in range (across-track) and 87 m in azimuth (along-track).

Radarsat-2 SAR has more imaging modes than Sentinel-1, but the TCVA processing unit solely uses SCANSAR Wide (SCW) imaging mode from Radarsat-2 mission. This mode has incidence angles ranging from 20 to 49 degrees and a resolution of about 100 m in both range and azimuth directions.

These wide swath modes allow acquisitions in dual-polarization, two images being acquired over the same area at the same time. One is in co-polarization (VV or HH) and one is in cross-polarization

(VH or HV). In this study we only use L1 data acquired in dual-polarization (VV+VH) to take benefit of the two polarization channels for the SAR wind retrieval (Mouche et al., 2017). An example of two simultaneous of Sentinel-1B SAR acquisitions with VV and VH polarizations over Veronica tropical cyclone in the South-Indian ocean close to the Australian coasts the 23rd of March 2019 between 21:38:33 and 21:39:52 UTC is presented on figure 2.1.

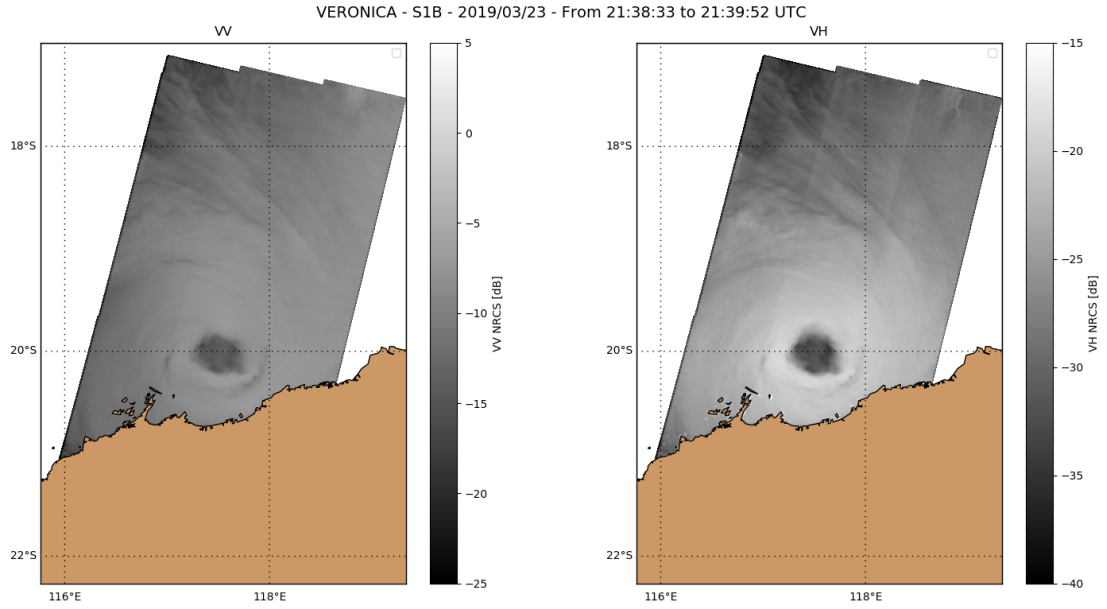

Figure 2.1: Example of Sentinel-1B SAR acquisitions over Veronica tropical cyclone on 2019-03-23 between 21:38:33 and 21:39:52 UTC. Left: Radar cross-section map in co-polarization (VV). Right: Radar cross-section map in cross-polarization (VH).

2.2.2. Acquisition strategy

Obtaining SAR observations over the eye of a tropical cyclone using the Sentinel-1 and RADARSAT-2 systems requires a specific strategy. Unlike weather satellites in geostationary orbit, which can image an entire hemisphere continuously every 10–15 minutes, satellite-based SAR instruments acquire data with a limited footprint. Also, SAR can acquire data during only about 30% of every orbit because of the radar's power requirements and the large data volume that must be downlinked. This why SAR data collections must be programmed in advance. For instance, in the case of Sentinel-1, a high level operation plan exists to set up the default acquisition strategy that ensures a background and optimal acquisition plan to serve Copernicus objectives. To maximize the number of SAR observations over Tropical Cyclone, a specific approach based on Tropical Cyclone forecast tracks has been set up to update the Sentinel-1 default acquisition plan and order Radarsat-2 data 3-5 days in advance. This strategy inherits from the hurricane watch program (Banal et al., 2007) and is called SHOC for Satellite Hurricane Observation Campaign (Mouche et al., 2019; Jackson et al., 2021).

In fact, collection opportunities are identified by comparing forecast storm tracks against possible SAR time or spatial footprints to trigger the data ordering to ESA and MDA and thus to possibly complete the Sentinel-1 standard collection pattern (sometimes fortuitously acquires imagery over tropical systems before explicit planning is enacted). These opportunities turns into SAR acquisitions over TC depending on the missions capabilities and objectives but also on the quality of the TC forecast track.

As of today, SHOC has allowed to collect more than 400 synoptic scenes of Tropical Cyclones (category 1 and stronger) worldwide. This collection is the core of the CyclObs archive database. The location and time of these observations are respectively shown for the 3 sensors on the map and bar plot, presented Figure 2.2. Amount/Percentage of SAR acquisitions per storm category, oceanic basin and sensors are also presented in pie charts.

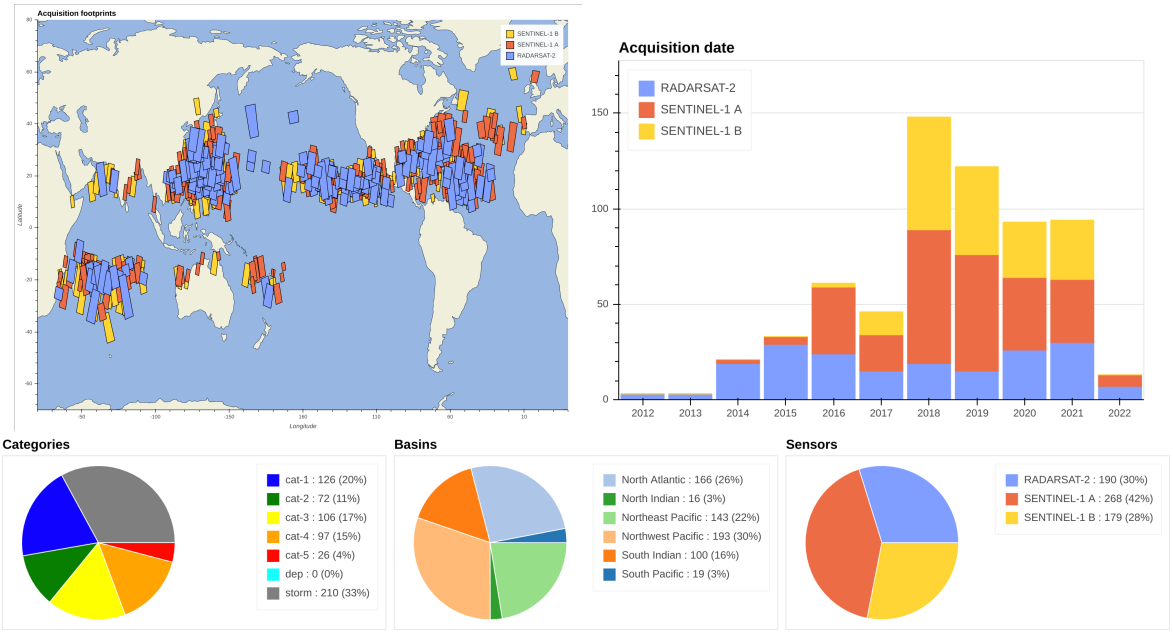

Figure 2.2: CyclObs statistics database. Top left: Map with acquisition location with respect to sensor (see color code). Top right: Time of acquisition with respect to sensor (see color code). Bottom : Amount/Percentage of SAR acquisitions per storm category (left), oceanic basin (middle) and sensors (right).

2.3. Level-2 CyclObs wind products

Level-2 CyclObs wind product main variable is the wind speed. A Level-2 CyclObs wind product can be composed of several successive Level-1 SAR acquisitions. Each Level-1 acquisition is processed into a Level-2 wind product. These products are then concatenated into a single Level-2 product. The wind can be processed at different resolutions from 1 to 50 km with a 1 km pixel spacing.

There are two versions of the product

- SAR Ocean Surface Wind along track (or swath) Level-2 product based on Radarsat-2, Sentinel-1A and Sentinel-1B measurements.
- SAR Ocean Surface Wind gridded Level-2 product based on Radarsat-2, Sentinel-1A and Sentinel-1B measurements

The TCVA processing chain relies on both the along-track and gridded Level-2 product at 3 km resolution.

The wind estimate relies on the use of both VV and VH channels. VV-NRCS is known to be very robust for wind vector estimates from low to high wind regimes, with low signal-to-noise ratio and sensitivity to ocean wind direction. Whereas VV-NRCS sensitivity is decreasing under more extreme conditions, VH-NRCS still exhibits significant sensitivity (Zhang and Perrie, 2012). Algorithm for Level-2 CyclObs wind product combines SAR information with a priori information. VV-NRCS and VH-NRCS measurements are combined with ocean wind vector from ECWMF (spatial resolution is 0.125° with a time step of 3 h) to provide a wind speed estimate. Gaussian errors are considered for observations, geophysical model function (GMF) used to relate NRCS to wind speed and direction as a function of radar parameters, and the model information. This leads to a minimization problem for the determination of the maximum probability to get a wind vector (speed and direction). For each NRCS measurements couple (VH and VV), the cost function to minimize writes:

$$J(u_{10}, v_{10}) = \sum_{\text{pp}\in[\text{VV,VH}]} \left[\frac{\sigma_0^{\text{pp}} - \text{GMF}^{\text{pp}}(\theta, \phi, U_{10})}{\Delta\sigma_0^{\text{pp}}}\right]^2 + \left[\frac{u_{10}^{apriori} - u_{10}}{\Delta u_{10}}\right]^2 + \left[\frac{v_{10}^{apriori} - v_{10}}{\Delta v_{10}}\right]^2, \quad (2.1)$$

where $\{u_{10}, v_{10}\}$ defines the space of solution in the geographical referential from -80 to 80 m/s and $\{\Delta u_{10}, \Delta v_{10}\}$, the associated errors. $u_{10}^{apriori}$ and $v_{10}^{apriori}$ are the *a priori* solution given by ECMWF model.

σ_0^{pp} and $\Delta\sigma_0^{pp}$ are respectively the NRCS measurements in co- (pp $=$ VV) and cross- (pp $=$ VH) polarization and the associated errors. $\text{GMF}^{pp}(\theta, \phi, U_{10})$ stands for the GMF defined for each polarization with respect to incidence angle θ, wind direction relative the antenna look direction ϕ and wind speed U_{10}. Figure 2.3 provides an example of CyclObs Level-2 SAR ocean surface wind speed map for Veronica TC obtained from Level-1 observations presented on Figure 2.1.

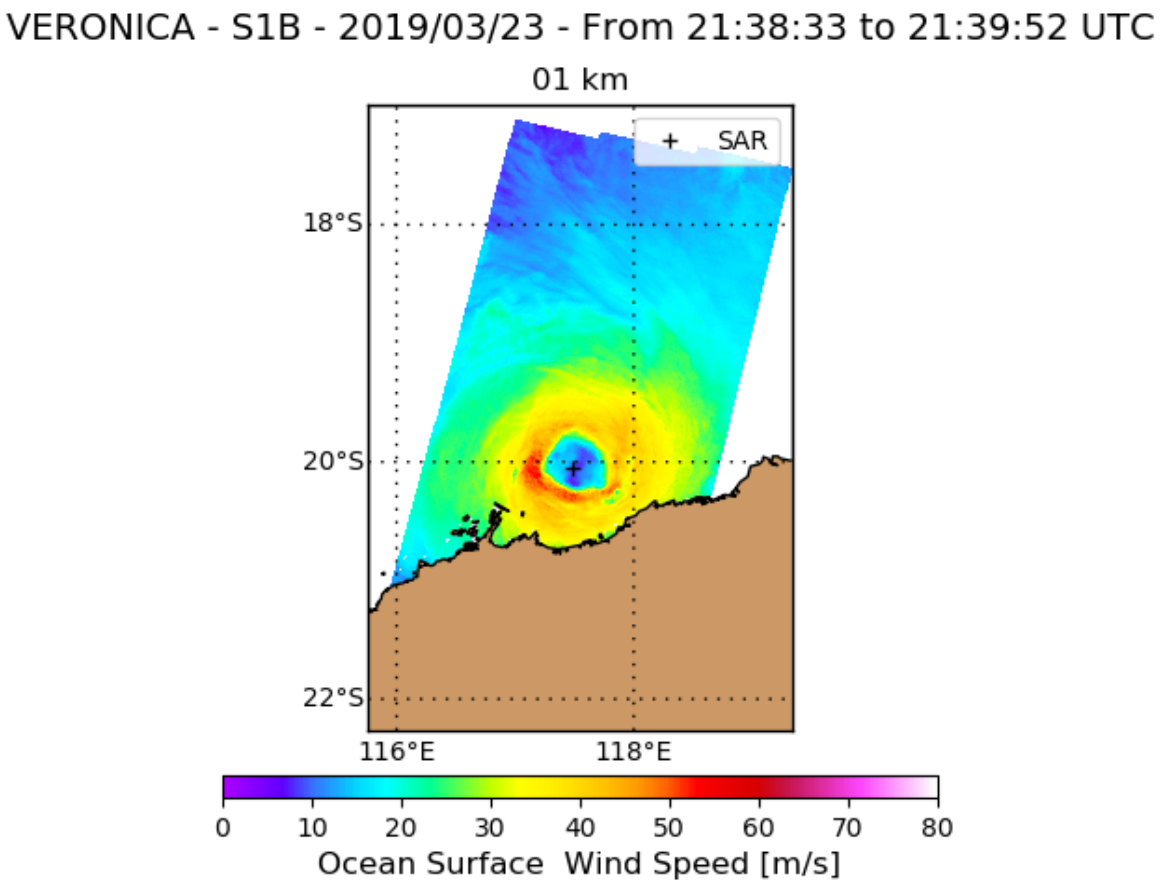

Figure 2.3: Example of CyclObs Level-2 ocean surface wind speed obtained from Sentinel-1B SAR acquisitions in dual polarization over Veronica tropical cyclone on 2019-03-23 as presented on Figure 2.1

3

Tropical Cyclone Vortex Analysis product overview

This chapter provides an overview of the Tropical Cyclone Vortex Analysis product and processing chain.

3.1. Product family

The TCVA product has 6 different sub-products

- 2 TC FIX product in csv-like ASCII format (.dat),
- 4 gridded products in netCDF format.

3.1.1. FIX products

The 2 FIX products are :

- per-acquisition TC FIX file : A TC FIX product is processed and delivered for each SAR acquisition over a TC.
- per-storm TC FIX file : This product regroups all per-acquisition TC FIX corresponding to the same storm in the one single file.

3.1.2. Gridded products

The 4 gridded products are :

- Cartesian grid product in geographical coordinates
- Cartesian grid product in tropical cyclone coordinates
- Polar grid product in geographical coordinates
- Polar grid product in tropical cyclone coordinates

Gridded products are in netCDF format. They contain two kinds of variables

- *Gridded data variables:* They are the same as the L2 C-Band SAR source file but they are regridded and rotated (for TC oriented products).
- *Analysis variables*: They are computed during TC Vortex Analysis process, they do not contain gridded data but rather scalar values or flags.

3.2. High Level processing flowchart

The TCVA processor uses as input Level-2 SAR wind products and TC tracks. In the processing unit, each Level-2 SAR wind product is associated to a TC and analyzed to extract TC parameters. The results are stored in the product family described in section 3.1. The main inputs and outputs of the

TCVA processor are described in the flowchart 3.1. Details about the processing unit are given in section 4

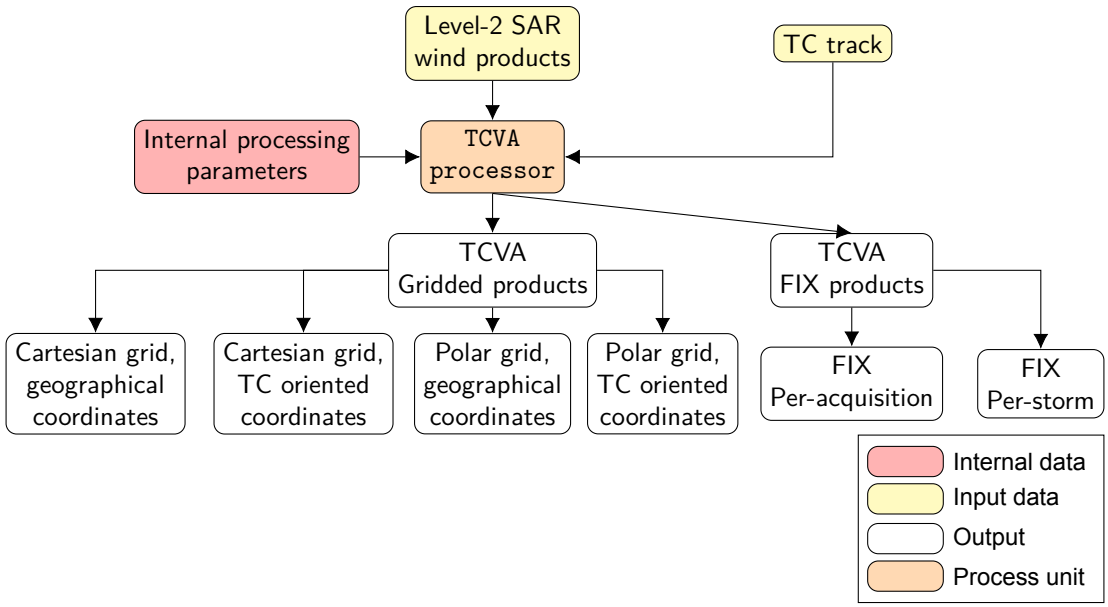

Figure 3.1: High level flowchart of the Tropical Cyclone Vortex Analysis processor interfaces.

The TCVA processing system needs the following inputs.

1. Input data
    - Level-2 SAR wind products are SAR Ocean Surface Wind along track and gridded Level-2 products, presented in the previous chapter and further described in Section 4.1.1.1,
    - C-Band SAR L2 meta-data from CyclObs database, as described in Section 4.1.1.2,
    - TC track used are Tropical Cyclone tracks from ATCF, as described in Section 4.1.1.3.
2. Internal auxiliary data
    - Processing parameters file, as described in Section 4.1.2.1.

The output of the TCVA processing chain is a collection of products in netCDF or ASCII format. This family product is presented in section 3.1 and a detailed description of each of the product content is given in chapter 6.

4

Tropical Cyclone Vortex Analysis product algorithm description

A general view the algorithm flowchart with the 3 different processing steps of the processing unit is presented on figure 4.1 below. The following sections detail the input files needed for the algorithm and provide a functional description of each of the processing steps of the processing unit.

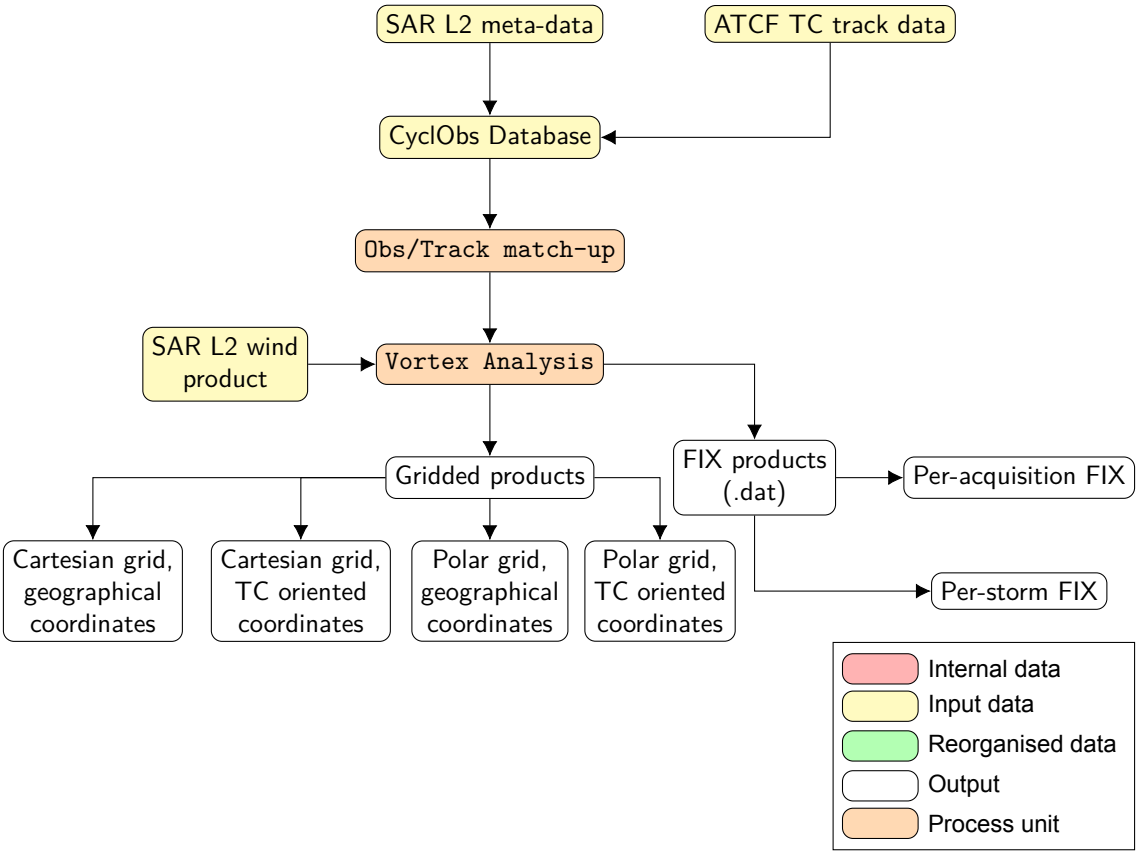

Figure 4.1: General flowchart of the algorithm. The color of cells detailed in the legend is kept for the other flowcharts in this document

4.1. Inputs files

4.1.1. Input data

SAR L2 wind product

SAR L2 product used as input of the processing are L2X concatenated C-Band SAR wind products. They are computed from Level-1 products from Sentinel-1 and Radarsat-2 missions and acquired in wide swath modes. L2X products results from the concatenation of L2 products. Each SAR ocean wind field corresponds to the instantaneous wind field measured at the SAR acquisition time.

Several L2X by-products are generated by the SARWING processing chain, two of them are used by the TCVA:

- The SARWING SWATH product is processed on a grid orientated along the satellite swath and regular in the image domain. Default resolution is 3 km and pixel spacing is 1 km. It is used for product generation as its data is the most faithful with the original acquisition.
- The SARWING GRIDDED product which is processed on a regular grid, in plate carrée projection (lat/lon). It is used for eye detection processing unit (described in Section 4.2.2) as it is more convenient to manipulate.

C-Band SAR L2 meta-data

The main C-Band SAR L2 meta-data are

- file location,
- acquisition geographic bounding box,
- timestamp of SAR acquisition

They are inserted into CyclObs database. Insertion of L2 meta-data into CyclObs database has multiple purposes, but a significant one (for TCVA but not only) is to perform automatic matchup with a TC track point.

ATCF track data

Tropical cyclone tracks and variables are obtained from ATCF (for The Automated Tropical Cyclone Forecasting System) best tracks (Sampson and Schrader, 2000). The best track data base contains spatial coordinates of tropical cyclones center location at 3 hours time resolution, and other variables such as maximum wind speed, wind radii, translation speed...

A wind radius is defined as the distance to the eye where the wind speed is equal to a specific value for a given geographical quadrant (NE, SE, SW, NW). For example R34 represents the distance to TC eye where the wind speed is equal to 34 kts. In the ATCF database, a wind radius corresponding to the 34, 50 and 64 kts is estimated for each of the four geographical quadrants. The radius of maximal winds (Rmax) is defined as the distance to eye where the wind speed reaches its maximum value in the TC. Figure 4.2 illustrates how these radii are connected to the wind field in the case of a idealized wind speed profile (Holland et al., 2010) in 1D (left) and in 2D (right).

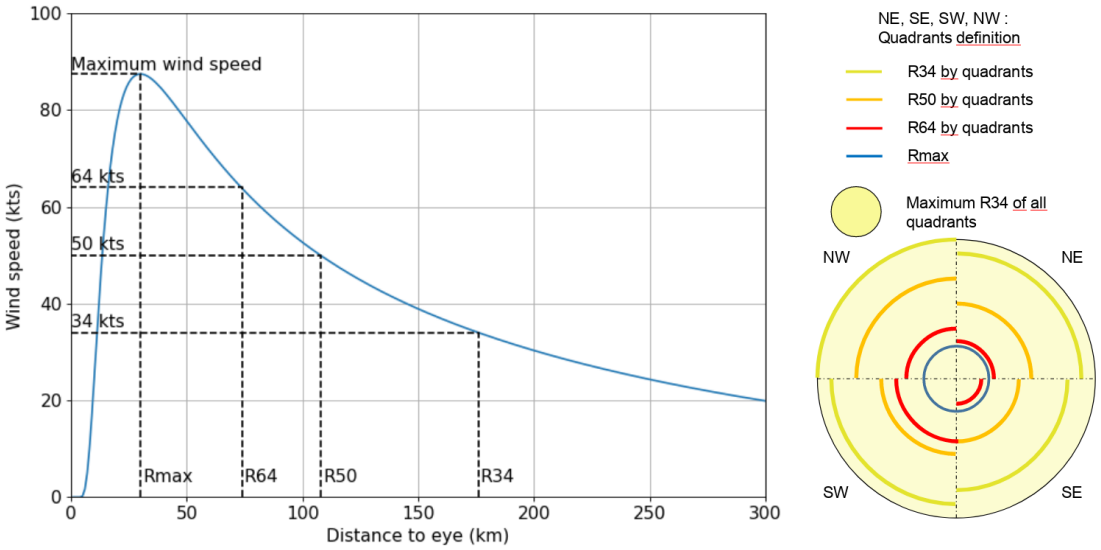

Figure 4.2: Left: Example of a theoretical wind speed profile (Holland et al., 2010) with respect to distance from the TC eye and associated wind radii for 34-knots (R34), 50-knots (R50), 64-knots (R64) and for the maximum wind speed (Rmax). Right: Example of R34, R50 and R64 wind radii for the 4 geographical quadrants values and Rmax as indicated in the ATCF.

An example of tropical cyclone track with its TC center locations, maximum wind speed and wind radii evolution is provided on figure 4.3 below. It shows that wind radii reach relatively different values depending on the geographical quadrant and the date. The distances between two successive 3-hours steps of the TC shows that the translation speed also varies. To recall, one of the goals of the TCVA product is to provide independent estimates of these variables from the SAR Level-2 wind products.

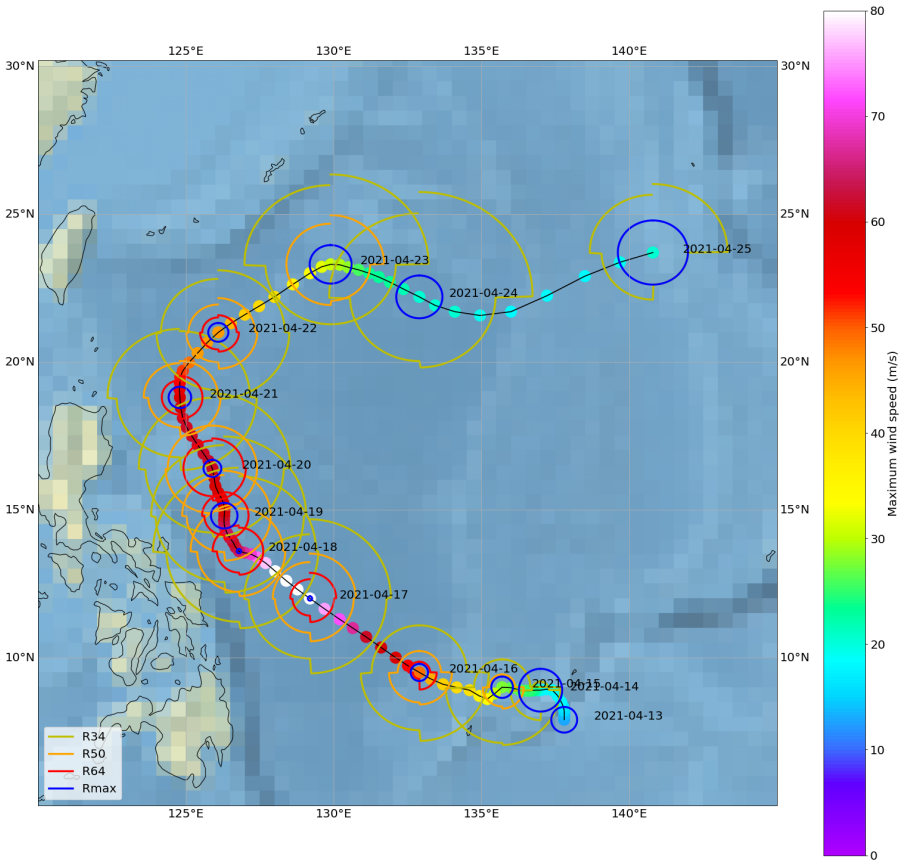

Figure 4.3: Track of tropical cyclone SURIGAE (April 2021). Temporal resolution of the track is 3 hours. Wind speed is colored at each step of the track. Wind radii are plotted by quadrant once a day

In the table below all names of variables used in this product are referenced.

Variable long name	Variable short name
Date of each track steps	t^{ATCF}
Longitude of each track step	lon^{ATCF}
Latitude of each track step	lat^{ATCF}
Maximum wind speed for each track step	$wind^{ATCF}$
34 kts wind radius for each track step (NE)	$r34_{ne}^{ATCF}$
50 kts wind radius for each track step (NE)	$r50_{ne}^{ATCF}$
64 kts wind radius for each track step (NE)	$r64_{ne}^{ATCF}$
34 kts wind radius for each track step (SE)	$r34_{se}^{ATCF}$
50 kts wind radius for each track step (SE)	$r50_{se}^{ATCF}$
64 kts wind radius for each track step (SE)	$r64_{se}^{ATCF}$
34 kts wind radius for each track step (SW)	$r34_{sw}^{ATCF}$
50 kts wind radius for each track step (SW)	$r50_{sw}^{ATCF}$
64 kts wind radius for each track step (SW)	$r64_{sw}^{ATCF}$
34 kts wind radius for each track step (NW)	$r34_{nw}^{ATCF}$
50 kts wind radius for each track step (NW)	$r50_{nw}^{ATCF}$
64 kts wind radius for each track step (NW)	$r64_{nw}^{ATCF}$
Maximum wind radius for each track step	rmw^{ATCF}
ATCF ID	id^{ATCF}
Basin along track	$basin^{ATCF}$

4.1.2. Internal auxiliary files

Processor parameters

In this section all the processing parameters of the algorithm and their impacts are detailed.

Observation/track matchup parameters See table.

Name	Symbol	Definition	Section	Default value
`track_sample_rate`	T_r	Integer to specify the interpolation rate, in minutes, for storm tracks before being inserted into database. For example, a value of 15 means that it will be interpolated to have 1 track point every 15 minutes.	4.2.1	`15`
`SAR_coloc_distance`	S_{cd}	Maximum distance, in meters, between the SAR acquisition bounding box and the track point, for the couple to be candidate for observation/track matchup.	4.2.1	`350 000`

Table 4.1: Processing parameters for SAR observation and TC track matchup.

TC Eye detection parameters See table.

name	Symbol	Definition	Section	Default value
`mask_radius_factor`	mr_f	Factor to multiply to the ATCF rmw to define the radius around the eye first guess (which is ATCF track point) in which the heterogeneity mask is not applied.	4.2.2.1	4
`research_radius_rmw_factor`	Rrmw_f	Factor to multiply to the ATCF rmw to define the radius around the eye first guess (ATCF track point) in which the high wind points are found to compute the high wind speed barycenter. The final research radius is $max(\text{Rrmw}_f * \text{rmw}, \text{Rr34}_f * r34)$	4.2.2.2	2
`research_radius_r34_factor`	Rr34_f	Factor to multiply to the ATCF r34 to define the radius around the eye first guess (ATCF track point) in which the high wind points are found to compute the high wind speed barycenter. The final research radius is $max(\text{Rrmw}_f * \text{rmw}, \text{Rr34}_f * r34)$	4.2.2.2	$1/2$
`low_wind_search_retry`	L_r	How many times modify the low wind research area radius until a valid low wind area barycenter is found.	4.2.2.2	10
`min_point_count`	M_p	Minimum point count on input C-Band SAR L2 data for the eye detection process unit to start.	4.2.2.1	3000
`fact_eye_shp`	E_f	Factor to extend or reduce the eye shape.	4.2.2.3	1

Table 4.2: Processing parameters for TC Eye detection.

Grid data parameters See table.

Name	Symbol	Definition	Section	Default value
`cart_resolution`	C_r	Resolution of cartesian grids	4.2.3.1	1000
`cart_grid_size`	C_s	`x` and `y` grid size for cartesian product	4.2.3.1	1000
`pol_inter_resolution`	P_r	Resolution for the intermediate cartesian grid that is converted to a polar grid.	4.2.3.1	1000
`pol_x_size`	P_{sx}	`x` grid size for the intermediate cartesian grid converted to polar.	4.2.3.1	1000
`pol_y_size`	P_{sy}	`y` grid size for the intermediate cartesian grid converted to polar.	4.2.3.1	1080
`pol_rad_reduce`	P_{rr}	Factor of division to downsample the polar rad grid from the previous size `pol_x_size` to its final product size.	4.2.3.4	2
`pol_theta_reduce`	P_{tr}	Factor of division to downsample the polar theta grid from the previous size `pol_y_size` to its final product size.	4.2.3.4	3
`max_polar_index_radius`	M_{pr}	Used to define the polar `rad` coordinate. $max(rad) = M_{\text{pr}} * P_r - P_r$. Also passed to opencv2 linearPolar maxRadius function parameter to indicate the circle radius.	4.2.3.4	500

Table 4.3: Processing parameters for data gridding.

4.2. Functional description

The following sections provide descriptions of some key algorithm parts.

A general view of the TCVA algorithm flowchart with the 4 different processing steps of the processing unit is presented on figure 4.4 below. The following sections detail the input data needed for the algorithm and provide a functional description of each of the processing steps of the processing unit.

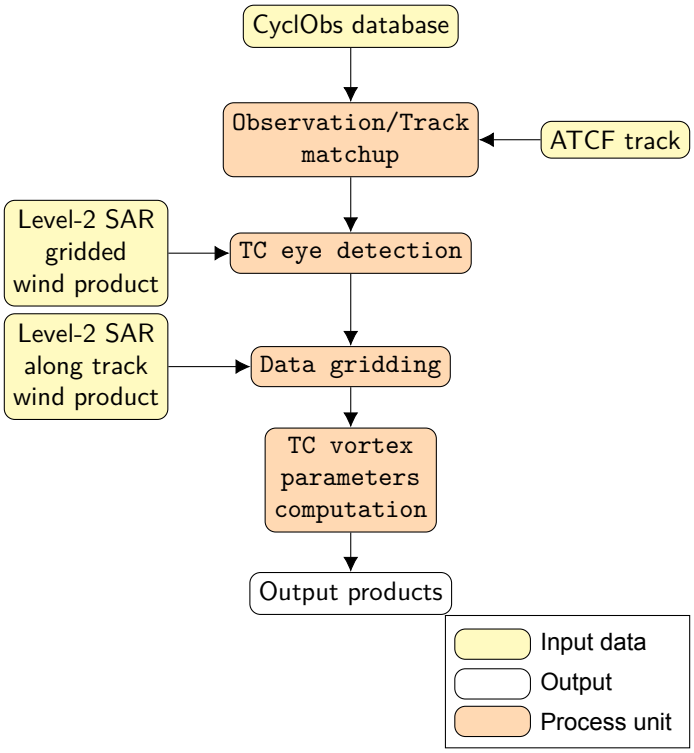

Figure 4.4: Flowchart of the Tropical Cyclone Vortex Analysis processing unit

4.2.1. SAR Observations and TC Track matchup

This section describes the observation/track matchup process unit, as shown on the figure 4.4

Observation and storm track matchup is an essential step in all CyclObs system. This step consists in matching up each satellite acquisition with a specific TC track point. The chosen track point is the spatio-temporally closest point.

Input variables for this step are SAR L2 wind products meta-data:

- acquisition timestamp t^{SAR},
- acquisition bounding box : $\text{lon}_{bb}^{\text{SAR}}$,$\text{lat}_{bb}^{\text{SAR}}$ = $\{\text{lon}_i; \text{lat}_i\}$, for $i \in [0, N_{\text{bb}}]$, where N_{bb} is the number of points in the bounding box.
- product file location,

and ATCF storm tracks interpolated key variables:

- timestamp t_j^{ATCF} for $j \in \left[0, N_{\text{times}}^{\text{interp}}\right]$,
- longitude,
- latitude,
- maximum sustained wind speed,
- radius of maximum wind speed
- all wind radii.

ATCF storm track are interpolated following `track_sample_rate` parameter described in table 4.1.2.1. Currently, the interpolation generates a track point every 15 minutes. Interpolation method is linear. The steps to get the matchup between this interpolated TC track and the SAR observations are:

1. We apply the following temporal criteria to find the collocated time stamp $t_{\text{coloc}}^{\text{ATCF}}$:

$$\Delta T_{[\text{SAR;TC}_{\text{track}}]} = \left|t^{\text{SAR}} - t_j^{\text{ATCF}}\right| < \texttt{track\_sample\_rate}/2, \tag{4.1}$$

where $N_{\text{times}}^{\text{interp}}$ is the number of interpolated timestamps in the TC track.

2. However, this steps can lead to SAR matchup with several different TC tracks. Typically, this can happens when several TC occur during the same dates. A matchup is considered valid if close enough to the SAR bounding box. The following spatial criteria is applied:

$$D_{[\mathrm{SAR;TC_{track}}]} = \mathrm{Dist}\left[(\mathrm{lon}_{bb}^{\mathrm{SAR}}, \mathrm{lat}_{bb}^{\mathrm{SAR}}); (\mathrm{lon}_{\mathrm{coloc}}^{\mathrm{ATCF}}, \mathrm{lat}_{\mathrm{coloc}}^{\mathrm{ATCF}})\right] < \texttt{SAR\_coloc\_distance} \quad (4.2)$$

3. After this step several different matchup can still exist, in cases where different TC track are close temporally and spatially. To chose a specific TC track among the remaining matchups, the one with the smallest distance $D_{[\mathrm{SAR;TC_{track}}]}$ and smallest temporal difference $\Delta T_{[\mathrm{SAR;TC_{track}}]}$ is selected.

Computed matchups are stored in CyclObs database table. CyclObs includes an API to query the CyclObs database and retrieve the matchups when needed for processing steps.

4.2.2. TC eye center detection

This section describes the TC eye center detection process unit, as shown on the figure 4.4

This unit uses the following CyclObs API outputs :

- L2 SAR product metadata (file location, timestamp, bounding box)
- Matched ATCF track point data (timestamp, location, radii, VMAX, RMAX)

L2 SAR wind product indicated by L2 meta-data is loaded in gridded format. The core eye detection analysis relies on the L2 product content.

The eye detection process unit produces the following outputs :

- Eye center longitude and latitude
- Eye shape

Also, several intermediate process variables are available as output, and included in the final TCVA product (further described in table 6.2.2.2) :

- Analyzed L2 file meta-data
- High wind speed research area
- Low wind speed research area
- High wind speed barycenter
- Low wind speed barycenter
- Eye first guess location
- Distance to coast
- Distance between first guess and acquisition bounding box border
- Area within 100km around track point outside acquisition bounding box
- Area of 100km around track point inside acquisition bounding box and on land
- Sum of `percent_outside` and `percent_inside_island` (variables described in **??**, which is the area of 100km around track point which is unusable for eye detection

The TC center research algorithm is performed on the 3-km wind fields. The procedure consists in three major steps.

1. A pre-processing is first carried out to prepare the image for extraction by associating it to the ATCF database, eliminating local outliers, and reducing the impact of rain and subswath artifacts.
2. A recursive TC center research is applied to find the TC's eye by searching for a low wind area near the maximum winds.
3. The eye-centered TC center position is retrieved by computing the eye shape.

To note, the criterion used here to define the final center position is thus its position inside the eye. This was considered as the logical definition (as it is the one an operator would visually assess), and the most suited for the assessment of local asymmetry which was one of the original purposes of this method used by Vinour et al. (2021). However, other definitions could be considered useful : for instance, a center computed with respect to the maximum wind ring instead of the eye shape would be more consistent to study the distribution of wind speed around the inner-core, and a center computed to maximize the average profile (i.e. centered with respect to the whole TC's symmetric structure) would be more suited for the computation of symmetric parametric profiles for instance.

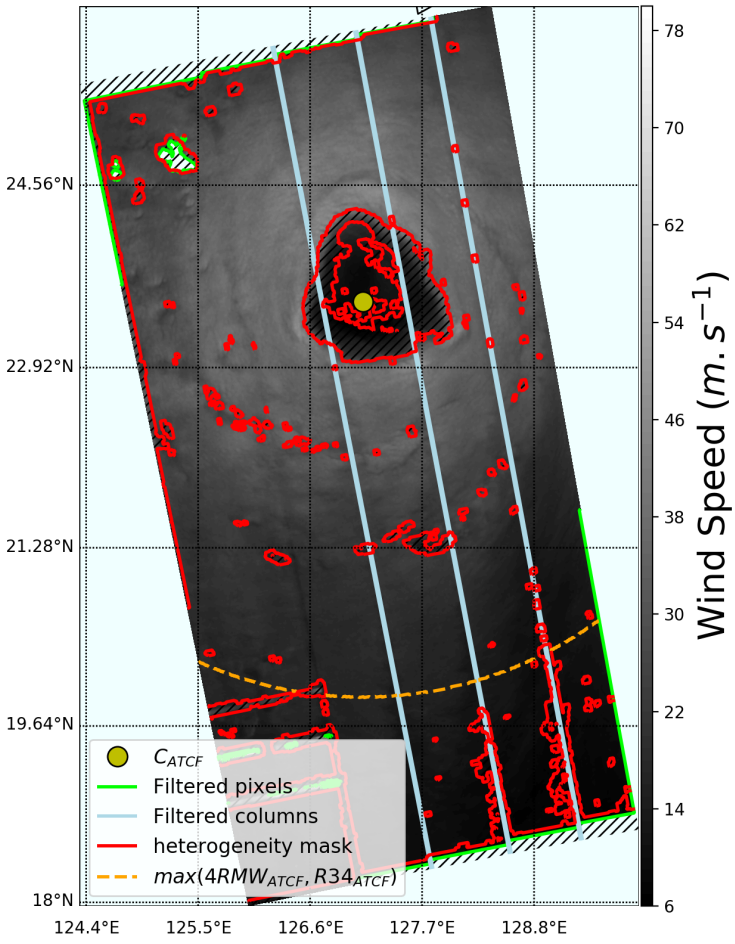

Figure 4.5: Illustration of the TC center research preprocessing step on the case of TC TRAMI (Western Pacific) observed with Sentinel-1 SAR on the 28th of September 2018. The L2 wind speed product is plotted along with the interpolated ATCF center C_{ATCF} (yellow dot), the MAD-filtered pixels (green contours) and columns (light blue lines), the heterogeneity mask (black hatched red contours) and the radius around C_{ATCF} above which the heterogeneity mask is applied (orange circle), equal to $\max(4 \times \text{RMW}^{\text{ATCF}}, \text{R34}^{\text{ATCF}})$.

Pre-processing
Only images containing at least `min_point_count` (default as 3000) wind speed data grid points are selected for the TC center research procedure : this empirical threshold is meant to reject all images with too many points on land, as land either causes local outliers (due to inland waters for instance) or prevents the procedure in cases where the TC has already reached landfall.

Outlier detection: Throughout the procedure, as SAR images are inherently impacted by local measurement errors, several filtering steps are applied to remove outliers from the wind field or from extracted signals and distributions. The filtering method applied is the Median Absolute Distribution (MAD) filter. Given a distribution of pixels x_i, outliers are defined as follows :

$$x_i = \text{outlier} \quad \text{when} \quad \frac{|x_i - \text{med}(x_i)|}{\text{MAD}_n} > \text{thr}, \tag{4.3}$$

where $\text{med}(x_i)$ is the median of the array pixels, $\text{MAD}_n = \text{med}(|x_i - \text{med}(x_i)|)$ is the MAD of the array, and thr is an arbitrary threshold value.

Image filtering and center first guess: Level 2 wind products are first prepared for the center research procedure through the following steps, illustrated on fig. 4.5 :

- the ATCF interpolated center position C_{ATCF} (yellow dot) is considered as a first guess for the TC center, and ATCF information such as the RMW (noted RMW^{ATCF}) or quadrants-averaged 34 knots radius (R34^{ATCF}) are considered as references for the TC size and hence used in the following steps
- A MAD filter is applied to the entire image to spot outlying pixels (green contours) caused by measurement errors that can impact the measurement and localization of maximum or minimum wind speeds. The MAD filter is applied with a very large threshold value of 50 to a grid containing for each pixel the difference between the wind speed of the pixel and the average wind speed among its direct neighbours. A similar method is applied to the column-wise averaged grid using a MAD filter threshold value of 10, this way masking subswath signatures that cause anomalously low or high wind values on entire grid columns (cf. light blue lines on fig. 4.5).
- The heterogeneity mask included in the L2 SAR product is also applied on the image (black hashed red contours), as it is designed to spot artifacts larger than isolated pixels, such as rainband signatures. These signatures can also disturb the center research procedure as they can generate erroneous low or high wind areas. The mask is however removed near the expected center location, in a radius of $\max(4 \times \text{RMW}^{\text{ATCF}}, \text{R34}^{\text{ATCF}})$ around the ATCF center (dotted orange circle). Indeed, although the heterogeneity mask is designed to mask rain-caused artifacts, it also often partially or entirely masks the eye-wall area, as this area contains very high local spatial wind speed gradients .

Once the image has been pre-processed to match the associated ATCF file and cleaned to remove or lower the impact of various measurement errors and artifacts, the center research procedure is applied.

Center research
The center research procedure designed here basically consists in the recursive computation of low wind areas centroids, and the search for a stable (i.e. invariant with recursions) low wind area near the area of maximum wind. Here, we assume that the TC eye is always characterized by much lower winds than its surroundings leading to distinctly formed eye. The procedure consists in the following steps, illustrated on Fig. 4.6.

- Starting from the first guess center C_{ATCF} (yellow dot), a research radius (yellow dotted cicle) is defined as

$$R_1 = \max(2 \times \text{RMW}^{\text{ATCF}}, \text{R34}^{\text{ATCF}}/2). \tag{4.4}$$

  The pixels lying inside R_1 with a wind speed higher than the 90% quantile of the wind speed distribution inside R_1 are extracted (magenta contours on fig. 4.6) and their centroid (barycenter)

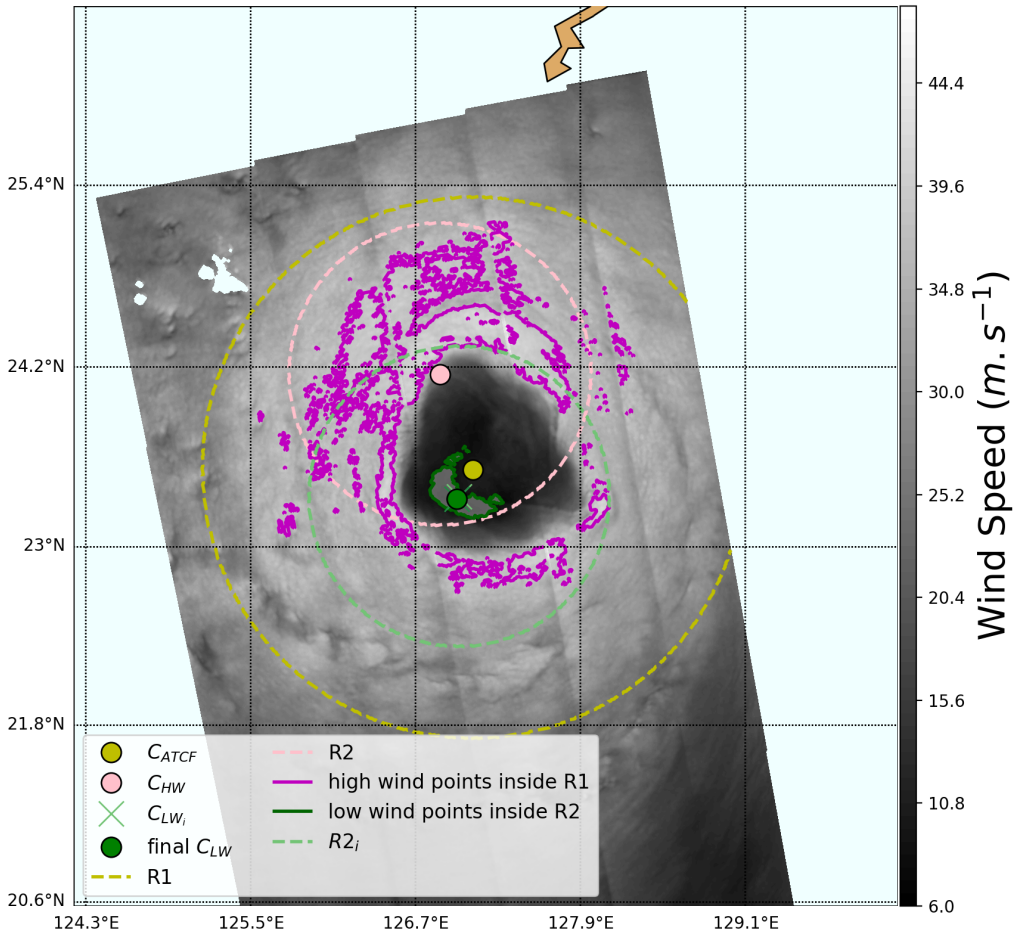

Figure 4.6: Illustration of the TC center recursive research method on the case of TC TRAMI (Western Pacific) observed with Sentinel-1 SAR on the 28th of September 2018. The ATCF center first guess C_{ATCF} is featured by a yellow dot, along with the first research radius R_1 (yellow dotted circle) inside of which the high wind pixels are located (magenta contours) and their centroid (barycenter) C_{HW} is computed (pink dot). This centroid is then used as the center of the second research radius R_2 (pink dotted circle), inside of which the lowest wind pixels are retrieved (dark green contours). The centroid of these pixels C_{LW_i} is then computed recursively (green crosses), until a stable position C_{LW} is found (dark green dot).

C_{HW} is computed (pink dot). This step allows to approach the TC center, which is necessary as the ATCF first guess is not necessarily close to the observed center due to the interpolation and possible inaccuracy in the TC track (for TC with very small eye for instance).

- This second guess based on the highest winds is used as the origin of the recursive research procedure. A smaller (because we expect to be closer to the TC eye center) research radius (green dotted circle on fig. 4.6) is defined as:

$$R_2 = \max(R_1/2, 1.5 \times ||C_{ATCF} - C_{HW}||). \tag{4.5}$$

The distance between C_{ATCF} and C_{HW} has been introduced because in some images (notably weak TCs with strong asymmetric rainbands), the C_{HW} center can be located very far from the actual eye of the storm. In such cases, basing the research radius only on ATCF issued parameters as R_1 can lead to an underestimation of the research radius and prevent center retrieval. Inside the circle defined by its radius R_2 and center C_{HW}, the centroid of low wind pixels C_{LW} (i.e. where the wind speed is lower than 5% of wind speeds inside the circle, shown by green contours on fig. 4.6) is retrieved.

- In order to ensure that the computed low wind centroid is located in the eye and not in the outer-core of the TC, the previous step is repeated several times (up to 10 times, defined by processing parameter `low_wind_search_retry`), each time starting from the latest found C_{LW_i} (the locations of these successive C_{LW_i} are denoted by green crosses on fig. 4.6). All C_{LW_i} positions are stored and, if a new C_{LW_i} is found to be already among the stored values, it is kept as the final center (i.e. the green dot on fig. 4.6).

As a summary, this recursive procedure is thus supposed to work as follows : starting from the high wind area located near the eye, the algorithm locates lowest winds which occur in majority inside the eye, and thus the C_{LW} is located in the eye; after a few iterations, as the circle of research almost does not change anymore, the computed centroids will eventually hit a point inside the eye two times, thus leading to a TC eye center guess.

Several configurations can however prevent this procedure from achieving the retrieval of the actual observed TC center. Indeed, if for some reasons one of the computed C_{LW_i} lies outside of the eye, the recursive procedure and the radial decrease of wind speeds in the TC will lead the following C_{LW_i} to be found each time further away from the center. Such situations can occur for different reasons. The principal ones are:

- The measured wind speed in the eye is not low enough with respect to surrounding outer-core winds
- The R_2 research radius is too large and thus encompasses low winds located at large radii from the center
- A large rainband places the C_{HW} far from the center and thus also leads to low winds located in the outer-core instead of the eye.

Either way, this leads the recursive procedure to exceed the maximum number of iterations (10), or to follow the decreasing radial wind profile until finding a stable point in the far outer-core of the TC.

To overcome this issue, an additional recursion was added to the method based on the distance between the final C_{LW} position and the two reference centers C_{ATCF} and C_{HW}. If

$$\min(||C_{LW} - C_{ATCF}||, ||C_{LW} - C_{HW}||) > R_1/2,$$

the recursive procedure is started over from the C_{HW} first guess with a reduced research radius of $0.8 \times R_2$. This test is reproduced up to 10 times (proc. parameter: `low_wind_search_retry`) until the computed C_{LW} position satisfies the condition. If `low_wind_search_retry` (10) repetitions are reached without finding a stable wind minimum close enough to the high wind area or ATCF center, the procedure issues an error and the center is set to its default ATCF value (i.e. the algorithm failed). This additional recursion usually allows to get rid of any original overestimation of R_2 and to narrow the research area of low wind pixels closer to the eye when necessary, yielding a satisfying TC center position located inside the eye. Once the eye position is located, the heterogeneity mask, which was applied during pre-processing but only for radii larger than $\max(2 \times RMW_{ATCF}, R34_{ATCF}/2)$ around the ATCF center, is re-applied around the found C_{LW} at radii larger than R_1, leaving the eye unmasked but masking rainband artifacts in the close vicinity of the eyewall.

Re-centering post-processing algorithm

The recursive procedure described above allows to locate the center inside the eye in most of the cases we have tested. However, this does not ensure that the position is located in the center of the eye : in several cases, especially when the eye is distorted, the distribution of wind is not uniform inside the eye, causing C_{LW} to be off-centered. This issue can be quite impacting for computations of azimuthal parameters (i.e. R34 by quadrant for instance) or azimuthally-averaged properties (such as the radial mean wind profile).

A re-centering method is thus applied, which relies on the extraction of the eye shape contour around the C_{LW} found previously, and the computation of its centroid. The eye shape extraction algorithm has been defined to be generic and can be applied to any SAR image for any TC category. Thus, it has to take into account the variability of TC eye situations (e.g. strongly asymmetric wind speed distributions, broken or distorted eyewalls, or secondary eyewalls and local wind maxima inside the eye) and potential SAR-associated errors and specificities (such as overestimated wind speeds in the eye for instance). The variety of configurations impedes the use of usual eye shaping method such as the method described by Zheng et al. (2017) which uses the PDF distribution in the near-eye area to find the wind speed associated to the eye shape contour : such straightforward method works fine on most cases with a well-formed eye and regular wind distribution around the eye, but is much less efficient when the TC is highly asymmetric.

The method designed here is thus more complex, but suited for a wider variety of cases : it consists in establishing a list of wind speed values suited for an estimation of the eye shape contour, and automatically selecting the best contour among these choices. The different steps are detailed hereafter, and illustrated on fig. 4.7.

Polar projection: The cartesian grid is first projected on a regular polar grid with an arbitrary size of 300 radial (r) by 360 azimuth (θ) points.

Determination of eye shape contours boundary values: Between the center of the grid and the radius of maximum wind for each azimuth RMW_θ, 10 closed contours are extracted for 10 values of wind speed (red contours on fig. 4.7). These values are based on the radial profiles extracted at high wind azimuths θ_{HW} containing wind speeds above the 99.5% quantile of the polar projected field (these azimuths are shown on fig. 4.7 as magenta dotted lines).

For each θ_{HW_i} among high wind azimuths θ_{HW}, the radial profile is smoothed and the wind speed corresponding to the radius of maximum wind speed radial gradient (denoted by white squares on fig. 4.7) is computed :

$$V_{\max\{dV/dr\}}\big|_{\theta_{HW_i}} = V(r|_{dV/dr=\max(dV/dr)})\big|_{\theta_{HW_i}}, \text{for } r < RMW_{\theta_{HW_i}} \tag{4.6}$$

where r is the radius and dV/dr is the radial gradient of wind speed. The average wind speed of maximum radial gradient $V_{\max\{dV/dr\}}\big|_{\theta_{HW}}$ is then computed by averaging over all θ_{HW_i}.

Likewise, for each θ_{HW_i}, the first decile (10% quantile) of the radial wind speed distribution between the center and RMW_θ is computed :

$$V_{D1\{V(r)\}}\big|_{\theta_{HW_i}} = V(r|_{V(r)-D1\{V(r)\}=\min(V(r)-D1\{V(r)\})})\big|_{\theta_{HW_i}}, \text{for } r < RMW_{\theta_{HW_i}} \tag{4.7}$$

where $D1\{V(r)\}$ is the first decile of the $V(r)$ wind speed distribution. The average corresponding wind speed $V_{D1\{V(r)\}}\big|_{\theta_{HW}}$ is retrieved.

Extraction of wind contours: 10 wind contours (pink contours on fig. 4.7) are then extracted based on a regular range of 10 wind speeds $V_{ref_{k\in[1,10]}}$ between $V_{D1\{V(r)\}}\big|_{\theta_{HW}}$ and $V_{\max\{dV/dr\}}\big|_{\theta_{HW}}$. For a given wind value V_{ref_k}, the contour $R_k(\theta)$ is defined as :

$$R_k(\theta) = \left\langle R_\theta(r) \right\rangle_r, \text{where } (r < RMW_\theta) \cup (||V_{ref_k} - V_\theta(r)|| < 1.0) \tag{4.8}$$

where $R_\theta(r)$ and $V_\theta(r)$ are the distributions of radius and wind speed at azimuth θ.

In order to avoid the sub-sampling of wind values caused by the coarse radial definition of the polar grid that could prevent the detection of matching $R_\theta(r)$, the radial profile $V_\theta(r)$ is interpolated on a

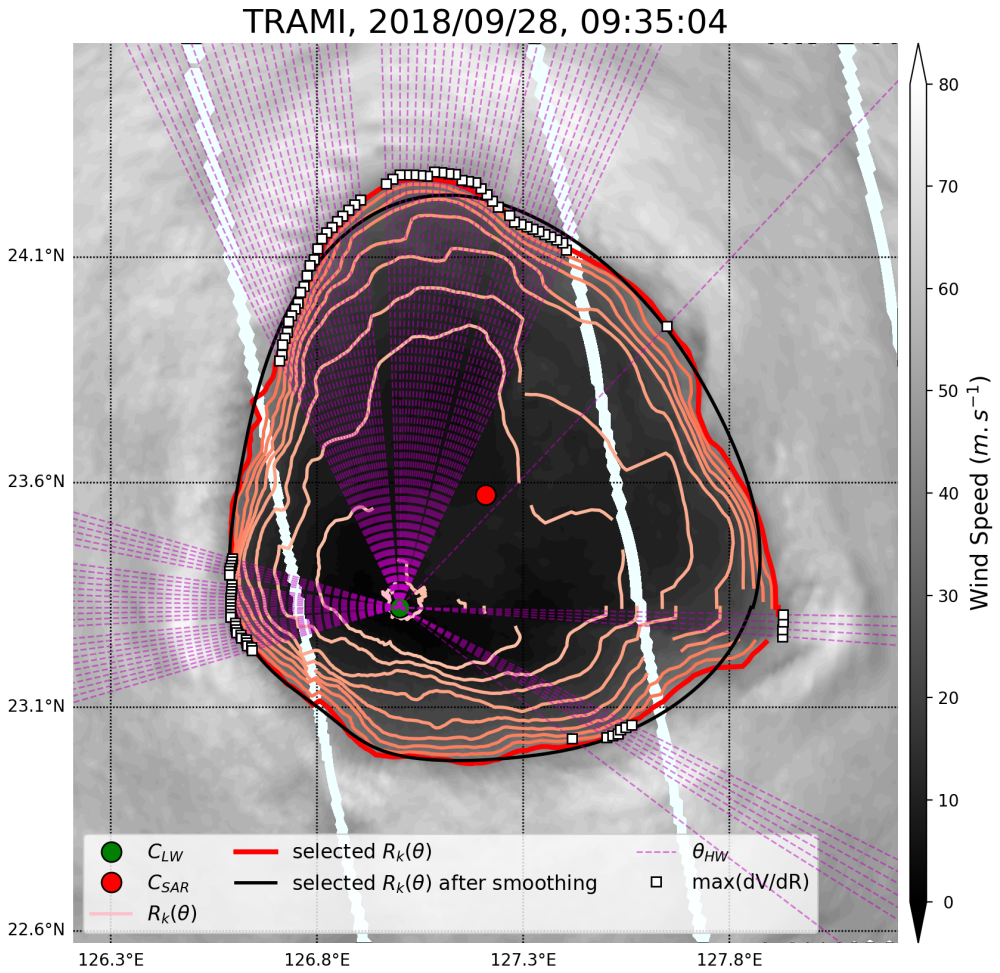

Figure 4.7: Illustration of the TC center re-centering step on the case of TC TRAMI (Western Pacific) observed with Sentinel-1 SAR on the 28th of September 2018. The low wind pixels barycenter output from the recursive method C_{LW} is shown by a dark green dot. High wind azimuths θ_{HW} are denoted by magenta thin dotted lines and, for each of these θ_{HW_i}, the radius corresponding to the maximum wind radial gradient max(dV/dR) is denoted by a white square. Pink thin lines show the 10 partially masked estimated contours $R_k(\theta)$. The final selected eye shape estimate is denoted by the thick red line, and the black line shows the same contour after applying the Butterworth filter for smoothing and completion of the contour. The final TC center estimate, C_{SAR}, is denoted by the red dot.

refined radius vector with 3000 points instead of 300. For each of the 10 reference wind speeds V_{ref_k}, an azimuthal distribution of radii $R_k(\theta)$ matching V_{ref_k} is thus extracted. These distributions are partially masked at azimuths where no match was found between the refined $V_\theta(r)$ distribution and V_{ref_k}.

Contour ranking and final selection: The 10 extracted wind contours are then compared to determine the best eye shape. The criteria considered to choose the best contour $R_k(\theta)$ are :

- the rank k of the $R_k(\theta)$, i.e. its distance from the center (a high rank is favored to encompass a large portion of the eye).
- the standard deviation rank k_{σ_R} of the contour, i.e. the index of $R_k(\theta)$ in the sorted distribution of $\sigma(R_k(\theta))$ (a low deviation is favored to avoid distorted shapes)
- the gradient standard deviation rank $k_{\sigma_{\partial R}}$ of the contour, i.e. the index of $R_k(\theta)$ in the sorted distribution of $\sigma(\frac{\partial R_k}{\partial \theta}(\theta))$ (a low deviation is favored to avoid local bumps in the signal and select smoother shapes)

For each contour, a score $S(k)$ is computed based on these two criteria as:

$$S(k) = 10 - k + k_\sigma + k_{\sigma_{\partial R}} \tag{4.9}$$

Finally, the contour $R_k(\theta)$ with the lowest score is taken among all contours with at least 70% unmasked points. In case no contour has more than 70% of data, the proportion of unmasked points is lowered to 50%, and if no contour is at least half unmasked, no eye shape is retained and the eye shape retrieval is abandoned.

Once the best eye shape contour $R_k(\theta)$ (large red contour on fig. 4.7) has been retrieved, it is linearly interpolated and filtered to yield a smooth eye shape $R_{\text{es}}(\theta)$ with no masked value (black contour on fig. 4.7). The filter applied is a Butterworth filter with a cutoff frequency corresponding to 40% of the signal explained variance, computed beforehand from the cumulative power spectrum of the signal. The centroid of this smoothed shape is computed and kept as the final TC center estimate C_{SAR} (red dot on fig. 4.7). In cases where the eye shape centroid falls outside of the polygon (which can happen when the eye is distorted and the polygon is concave), the final TC center is defined as the pole of inaccessibility of the polygon, i.e. the most distant internal point from the polygon outline.

TC center quality flag

For each TCVA product, a quality flag is associated to the TC center retrieved. In fact, this quality flag gathered several different quality flags to provide one single value :

- 0 means high confidence (good);
- 1 means medium confidence (warning)
- 2 mean low confidence (bad).

While the two FIX products only contains the TC center quality flag, all flags are included in the four gridded products. This section presents each of these flags and how there are combined together to built the TC center quality flag.

RMW inaccuracy: Several flags are computed with respect to the size of the eye. The RMW parameter is a good proxy for that. In fact, There are 4 flags that rely on TC RMW for their calculation. However, reported RMW in the TC tracks often suffers from inaccuracy (Combot et al., 2020). RMW is thus computed from Chavas and Knaff (2022) based on their empirical formula to define a new RMW, namely RMW_{CK22}, from the other ATCF TC tracks parameters :

$$\text{RMW}_{\text{CK22}} = (\text{Vmax}_{\text{ATCF}}/F_{\text{cor}})\left[\sqrt{1 + (2F_{\text{cor}} \times M_{\text{ratio}} \times M_{17})/(\text{Vmax}^2_{\text{ATCF}})} - 1\right] \tag{4.10}$$

where :

$$M_{17} = 17.5 \times 1000R_{17} + 0.5F_{\text{cor}}(1000R_{17}^2) \tag{4.11}$$

$$M_{\text{ratio}} = 0.482 \exp\left[0.00309(\text{Vmax}_{\text{ATCF}} - 17.5) + -0.00304(\text{Vmax}_{\text{ATCF}} - 17.5) \times 0.5 \times F_{\text{cor}} \times R_{17} \times 1000\right] \tag{4.12}$$

In these equations, R_{17} stands for R34^{ATCF}, the ATCF wind radii corresponding to 34 knots wind speed. F_{cor} is the coriolis force applied to the cyclone, intercept is ???????????, coef1 is ????????, coef2 is ??????????.

In spite of this new estimate of RMW, we noted that there are still some cases of large differences between RMW_{CK22} and SAR-derived RMW, namely RMW_{SAR}. By default RMW_{CK22} is used for flag computation. However, it may be largely inaccurate in some cases which can raise false bad flag values. To correct for this, the RMW_{CK22} is compared to the RMW_{SAR} (computed during TC center analysis). If $\text{RMW}_{\text{CK22}}/\text{RMW}_{\text{SAR}} > 1.4$ and both $\text{Vmax}_{\text{ATCF}}$ and $\text{Vmax}_{\text{ATCF}}$ indicate a TC at least category 1, then we consider RMW_{CK22} as unreliable, and use RMW_{SAR} instead for flag calculation. For the sake of simplicity, in the following we use RMW for the radius of maximum wind speed.

The different flags are detailed hereafter and Figure 4.8 indicates at which step these flags are computed.

First there are flags defined with respect to the consistency between acquisition swath limits and the ATCF TC tracks and with respect to the presence of land within the image footprint.

- **Track_Point_Flag:** This flag indicates if the closest 15-minutes interpolated ATCF track point is inside or outside the satellite acquisition bounding box.
  - if C_{ATCF} is outside, Track_Point_Flag is set to 2 (bad).
  - if C_{ATCF} is inside, Track_Point_Flag is set to 0 (good).
- **Distance_Track_Bbox_Flag:** This flag evaluates the distance between the closest 15-min interpolate ATCF track point C_{ATCF} and the closest bounding box border BBB. Being too close to the border is considered as an indicator of failure because the cyclone may not have been observed entirely. The distance is computed as follows

$$D_{C_{\text{ATCF}},\text{BBB}} = \min\Big(\text{Dist}(C_{\text{ATCF}}, \text{BBB})\Big) \tag{4.13}$$

  and used as:
  - if $D_{C_{\text{ATCF}},\text{BBB}} \leq 25000$, Distance_Track_Bbox_Flag is set to 2 (bad),
  - if $25000 < D_{C_{\text{ATCF}},\text{BBB}} \leq 40000$, Distance_Track_Bbox_Flag is set to 1 (warning),
  - if $D_{C_{\text{ATCF}},\text{BBB}} > 40000$, Distance_Track_Bbox_Flag is set to 0 (good).

  This flag is re-qualified depending on the Percent_Eye_Bbox_Flag. If Percent_Eye_Bbox_Flag is equal to 0 or 1, Distance_Track_Bbox_Flag is re-qualified from 1 to 0 or from 2 to 1.
- **Land_Flag:** This flag evaluates the quantity of land inside the high wind research area. Having land in this area can prevent from finding the TC eye because it is located over land and not ocean but also because the quality of the land mask can produce artefact of strong wind that impact the estimate of C_{HW}. The percentage of land within the area is computed :

$$P_{\text{Land}} = 100 \frac{\text{Area(Land)}}{\text{Area(Ocean)}}\bigg|_{\text{Area(HW)}}, \tag{4.14}$$

  where $\text{Area}(\text{HW})$ stands for the area of high wind speeds (used to compute C_{HW}). Flag values are defined as:
  - if $P_{\text{Land}} > 3\%$, Land_Flag is set to 2 (bad),
  - if $0.5\% \leq P_{\text{Land}} \leq 3\%$, Land_Flag is set to 1 (warning),
  - if $P_{\text{Land}} < 0.5\%$, Land_Flag is set to 0 (good).

Two flags are defined with respect to the high wind and low wind speeds barycenters:

- **Lwind_Hwind_Flag:** Lwind_Hwind_Flag evaluate the quality the barycenter of the low wind speeds area C_{LW} and the barycenter of the high wind speeds area C_{HW} as obtained from the SAR data analysis (see section 4.2.2.2) thanks to the computation of the distance between C_{LW} and C_{HW} normalized by RMW :

$$D_{\text{LWHW}} = \text{Dist}(C_{\text{LW}}, C_{\text{HW}})/\text{RMW} \tag{4.15}$$

  Considering that C_{LW} is close to the true TC center and C_{HW} is close to the location of the maximum wind speeed, D_{LWHW} is expected to be about 1 when the estimates of the two barycenters is optimal. Lwind_hwind_Flag is then defined such as:

  - if $D_{\text{LWHW}} \geq 1.7$, Lwind_hwind_Flag is set to 2 (bad),
  - if $1.6 \leq D_{\text{LWHW}} < 1.7$, Lwind_hwind_Flag is set to 1 (warning),
  - if $D_{\text{LWHW}} < 1.6$, Lwind_hwind_Flag is set to 0 (good).

  The threshold of 1.7 (larger than 1) has been chosen to take into account cases where a strong rain bands can disturb the evaluation of C_{HW} location (too far from the eyewall. see section XXX for an example).
- **Dist_Lwind_Flag:** Dist_Lwind_Flag is obtained by comparing the distance between the low wind speeds area barycenter C_{LW} and the SAR-derived TC center C_{SAR} with the TC RMW. The goal is to evaluate the quality of the re-centering post-processing algorithm (see section 4.2.2.3). In particular, it aims at flagging the cases where the eye-wall appears to be strongly elongated or incomplete possibly leading to a re-centering far from the initial TC center location indicated by the low wind speeds area (C_{LW}). Indeed, we expect that the distance between the C_{LW} and C_{SAR} to be less than the distance between the C_{SAR} and RMW. Here, the latter distance is approximated to 0.8*RMAX. The flag is thus based on the following distance:

$$D_{\text{LW}} = \text{Dist}(C_{\text{LW}}, C_{\text{SAR}})/\text{RMW} \tag{4.16}$$

  and defined such as

  - if $D_{\text{LW}} > 0.8$, Dist_Lwind_Flag is set to 2 (bad),
  - if $0.6 \geq D_{\text{LW}} > 0.8$, Dist_Lwind_Flag is set to 1 (warning),
  - if $D_{\text{LW}} < 0.6$, Dist_Lwind_Flag is set to 0 (good).

Then, there are flags defined to take into account for the location of the SAR-derived TC center location and TC eye extent with respect to the SAR swath limits:

- **Eye_Contained_Flag:** This flag indicates if the SAR-derived eye center C_{SAR} is inside or outside the satellite acquisition bounding box. In fact, the only processing step than can produce the SAR-derived TC center outside this bounding box is the re-centering (see section 4.2.2.3). The flag is defined by the following criteria:

  - if C_{SAR} is found outside the bounding box, Eye_Contained_Flag is set to 2 (bad),
  - if C_{SAR} is found outside the bounding box, Eye_Contained_Flag is set to 0 (good).
- **Distance_Center_Bbox_Flag:** This flag evaluates the distance between the SAR-derived TC center C_{SAR} and the closest bounding box border BBB. Being too close to the border is considered bad because this indicates that the cyclone eye could have been observed only partially. The distance is computed as follows

$$D_{C_{\text{SAR}},\text{BBB}} = \min\Big(\text{Dist}(C_{\text{SAR}}, \text{BBB})\Big) \tag{4.17}$$

  and used as:

  - if $D_{C_{\text{SAR}},\text{BBB}} \leq 25000$, Distance_Center_Bbox_Flag is set to 2 (bad),
  - if $25000 < D_{C_{\text{SAR}},\text{BBB}} \leq 40000$, Distance_Center_Bbox_Flag is set to 1 (warning),
  - if $D_{C_{\text{SAR}},\text{BBB}} > 40000$, Distance_Center_Bbox_Flag is set to 0 (good).

  This flag is re-qualified depending on the Percent_Eye_Bbox_Flag. If Percent_Eye_Bbox_Flag is equal to 0 or 1, Distance_Center_Bbox_Flag is re-qualified from 1 to 0 or from 2 to 1.
- **Percent_Eye_Bbox_Flag:** This flag evaluates the area of the eye shape outside the acquisition bounding box. In particular, this flag is used to re-qualify Distance_Track_Bbox_Flag and Distance_Center_Bbox_Flag flags (see after). The percentage of TC eye included in the bounding box is computed as:

$$P_{\text{Eye,BBB}} = 100\frac{\text{Area}(R_{\text{es}}(\theta)\big|_{\text{BBB}})}{\text{Area}(R_{\text{es}}(\theta))}, \tag{4.18}$$

  where $R_{\text{es}}(\theta)$ and $R_{\text{es}}(\theta)\big|_{\text{BBB}}$ stands for eye shape area and for the intersection area between the acquisition bounding box and the eye shape, respectively. $P_{\text{Eye,BBB}}$ is used to defined the Percent_Eye_Bbox_Flag such as :

- if $P_{\text{Eye,BBB}} \leq 70\%$, Percent_Eye_Bbox_Flag is set to 2 (bad),
- if $70\% < P_{\text{Eye,BBB}} < 80\%$, Percent_Eye_Bbox_Flag is set to 1 (warning)
- if if $P_{\text{Eye,BBB}} \geq 80\%$, Percent_Eye_Bbox_Flag is set to 0 (good).

Two flags are also defined with respect to the TC eye shape:

- **Eye_Length_Flag:** The Eye_Length_Flag is obtained by comparing the maximum radius of the eye shape $R_{\text{es}}(\theta)$ and the TC RMW :

$$R_{R_{\text{es}},RMW} = \max\big(R_{\text{es}}(\theta)\big)/\text{RMW} \tag{4.19}$$

  Eye_Length_Flag values are defined based on this ratio. When is too far from 1.0 the eye shape and thus the SAR-derived TC eye center are expected to be poor quality:

  - if $R_{R_{\text{es}},RMW} < 0.17$ or $R_{R_{\text{es}},RMW} > 1.2$, Eye_Length_Flag is set to 2 (bad),
  - if $0.17 < R_{R_{\text{es}},RMW} < 0.20$ or $1.0 < R_{R_{\text{es}},RMW} < 1.2$, Eye_Length_Flag is set to 1 (warning).
  - Else, Eye_Length_Flag is set to 0 (good).

- **Eye_Circularity_Flag:** This flag evaluates the eye shape $R_{\text{s}}(\theta)$ circularity. Here we assume that non-circular eye shape obtained with the proposed algorithm denotes cases where the eye is hardly discernable (even by an operator). These cases generally correspond to eye with asymetry, mixing, disturbed storms or storms in formation). TC experiencing an eye replacement cycle can also lead to an eye shape mixing the two eye-walls. The circularity of the eye shape can thus be used as an indicator of failure to detect the eye center. This flag, is based on the thinness ratio T_{eye} :

$$T_{\text{eye}} = \frac{4 * \pi * \text{Area}(R_{\text{es}}(\theta))}{\big[\text{Perimeter}(R_{\text{es}}(\theta)\big]^2} \tag{4.20}$$

  and defined such as

  - if $T_{\text{eye}} < 0.65$, Eye_Circularity_Flag is set to 2 (bad),
  - if $0.65 \leq T_{\text{eye}} < 0.75$, Eye_Circularity_Flag is set to 1 (warning),
  - if $T_{\text{eye}} \geq 0.75$, Eye_Circularity_Flag is set to 0 (good).

A flag is also defined with respect to the consistency between SAR-derived TC center and the IBTrACS TC center track:

- **Track_Flag:** Track_Flag evaluates the consistency between SAR-derived TC center and IBTrACS based on the distance between the SAR-derived TC center and the closest interpolated IBTrACs center.

$$D_{\text{RMW}} = \text{Dist}(C_{\text{SAR}}, C_{\text{IBTrACS}})/\text{RMW} \tag{4.21}$$

  Assuming that $D_{\text{RMW}} = 1$ means that the IBTrACS center is located right on the eye wall, then

  - if $D_{\text{RMW}} \geq 1.1$, the consistency between SAR-derived TC center and IBTrACS is considered bad and Track_Flag is set to 2 (bad),
  - if $0.8 \leq D_{\text{RMW}} < 1.1$, the consistency between SAR-derived TC center and IBTrACS is considered as warning and Track_Flag is set to 1 (warning),
  - if $D_{\text{RMW}} < 0.8$, the consistency between SAR-derived TC center and IBTrACS is considered good and Track_Flag is set to 0 (good).

Finally these flags are combined into one single flag:

- **Center_Quality_Flag:** This flag intends to summarize the information from other flags to give a overall indication of SAR-derived TC eye center location (C_{SAR}) quality. This is done through weighted sum S_W :

$$\begin{aligned} S_W &= 0.3 \times \text{Eye\_Length\_Flag} + 0.7 \times \text{Track\_Flag} + 0.5 \times \text{Lwind\_Hwind\_Flag} \\ &+ 0.4 \times \text{Dist\_Lwind\_Flag} + 0.9 \times \text{Eye\_Contained\_Flag} \\ &+ 0.25 \times \text{Distance\_Center\_Bbox\_Flag} + 0.25 \times \text{Distance\_Track\_Bbox\_Flag} \\ &+ 0.3 \times \text{Eye\_Circularity\_Flag} + 0.4 \times \text{Track\_Point\_Flag} + 0.9 \times \text{Land\_Flag} \end{aligned}$$

  - if $S_W \geq 2$, Center_Quality_Flag is set to 2 (bad)
  - if $1 \leq S_W < 2$, Center_Quality_Flag is set to 1 (warning),
  - if $S_W < 1$, Center_Quality_Flag is set to 0 (good)

4.2.3. Data gridding

This section describes the data gridding process unit.

The data gridding process unit uses as input the location of the TC eye center from the TC eye center detection unit and the SAR L2 along track (swath) product. The purpose of this unit is to use the L2 product content to build gridded data that are centered on the given TC eye center. Four grids are defined:

- Cartesian grid in geographical coordinates
- Cartesian grid in tropical cyclone coordinates
- Polar grid in geographical coordinates
- Polar grid in tropical cyclone coordinates

Those grids contains all variables from the L2 along track (swath) product. They are simply regridded and interpolated to fill gaps.

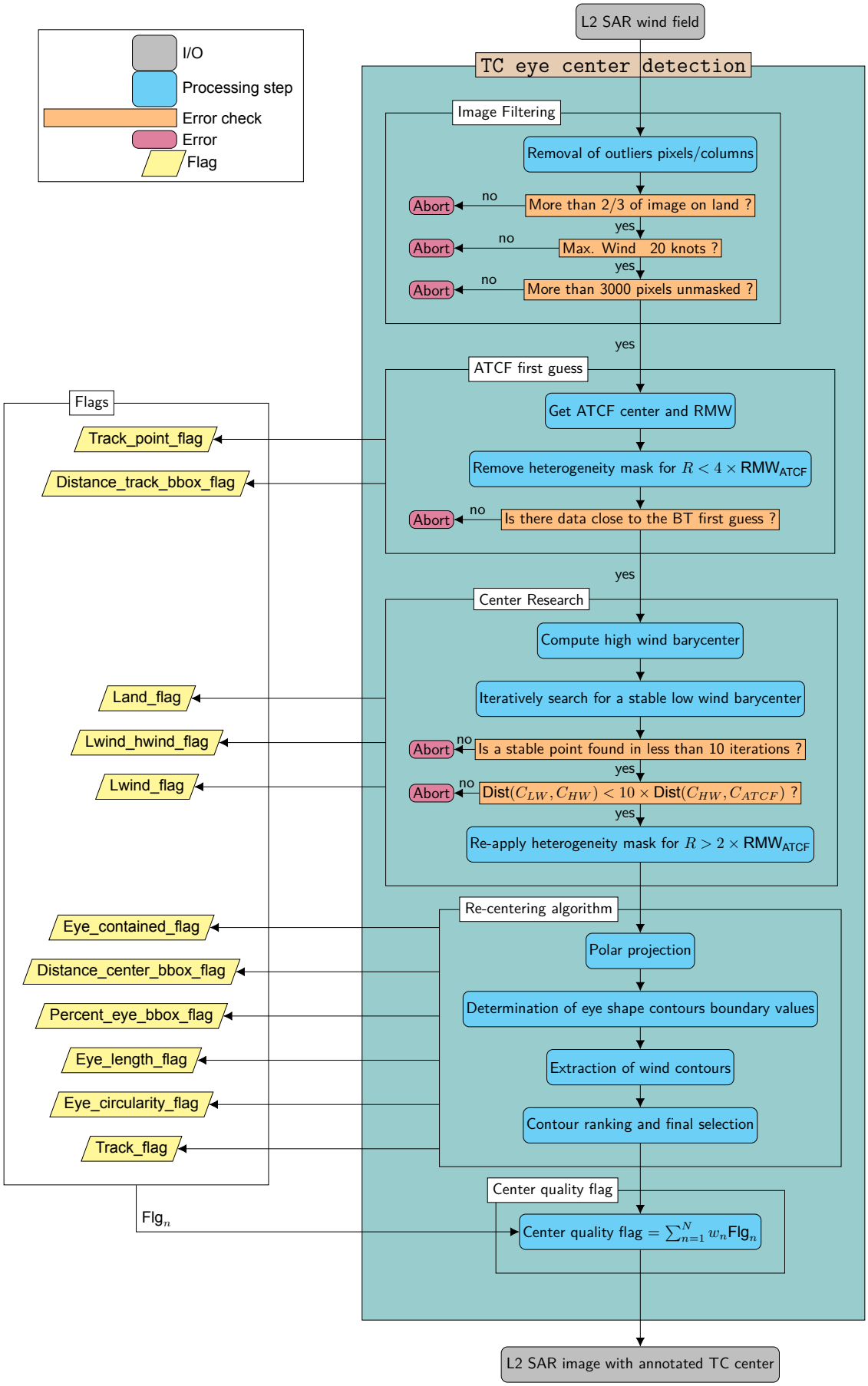

Figure 4.8: Flowchart of the Eye Research and Detection Algorithm

Overview of grid data process unit:

1. Open L2 along track (swath) product file, swath format (irregularly gridded)
2. Project the L2 data on a 1000x1000 grid in azimuthal equidistant projection (regular grid)
3. Project the L2 data on a 1000x1080 grid in azimuthal equidistant projection (regular grid), used for polar conversion
4. From the 1000x1080 azimuthal equidistant dataset, build a polar dataset, using opencv linearPolar function, giving a 1000x1080 grid. This grid is downsampled to 500x360.
5. Compute cyclone speed and direction using TC track points.
6. Rotate the polar dataset to match the cyclone direction (theta 0° = cyclone propagation direction).
7. Rotate the azimuthal equidistant 1000x1000 grid to match cyclone direction.
8. Add meridional and zonal wind speed components for north oriented dataset, and across track and along track for cyclone oriented ones.
9. Add radial and tangential wind speed components for cyclone oriented datasets.
10. Add inflow angle and parameterized inflow angle to cyclone oriented datasets.
11. Compute analysis variables
    - Compute wind radii (in knots/nmi and mps/km) with respect to geographical and tropical cyclone referentials.
    - Compute VMAX and RMAX.
12. Adding the various analysis variables to datasets.
13. Saving datasets to netCDF.

Building azimuthal equidistant grid centered on TC eye center
The L2 along track (swath) product file is defined on an irregular longitude/latitude grid with a resolution around 3 km. The TC eye center is used to create a regular grid centered on the TC eye center. Because of its accuracy, we chose an azimuthal equidistant grid as a coordinate grid.

This grid plays two roles :

- it is used as an intermediate grid that is then converted to polar coordinates.
- it is used as a final grid in two of our products (cartesian products).

In short, the operations consist in these steps:

1. Transform longitude and latitude grid from PlateCarre projection to azimuthal equidistant projection.
2. Create the coordinates grids ranging from -499 000 to 499 000 with a step of 1000.
3. Create two index arrays that will be used to assign from the original grid to the new one.
4. Filter indexes that are outside the destination grid
5. Assign data to new grid using index arrays
6. Interpolate data to fill gaps. Gaps appear because we interpolate from an irregular grid to a regular one, and because we change the projection.

Estimating cyclone speed and propagation direction
Estimating cyclone propagation direction is a necessary step to produce TC oriented products. Indeed it is needed to rotate our grids an have the product in the cyclone-oriented referential. Cyclone propagation speed is not use for the data gridding but it a key parameter to describe the cyclone current state. Speed and direction estimation is achieved using several TC track points. If enough track data is available (not true at the beginning and the end of the TC lifecyle), speed and direction is computed for 5 intervals (with t^{SAR} as satellite acquisition time):

- $I_1 = \left[t^{\text{SAR}} \text{ - 3 hours}; t^{\text{SAR}}\right]$
- $I_2 = \left[t^{\text{SAR}} \text{ - 6 hours}; t^{\text{SAR}}\right]$
- $I_3 = \left[t^{\text{SAR}} \text{ - 3 hours}; t^{\text{SAR}} \text{ + 3 hours}\right]$
- $I_4 = \left[t^{\text{SAR}}; t^{\text{SAR}} \text{ + 3 hours}\right]$

- $I_5 = \left[t^{\text{SAR}}; t^{\text{SAR}} + 6 \text{ hours}\right]$

The temporally closest track point is retrieved for each I_k interval bound and its timestamp and location are used to compute direction and speed, as:

$$T_{I_k} = t_{k_2}^{\text{ATCF}} - t_{k_1}^{\text{ATCF}} \tag{4.22}$$

$$D_{I_k} = \text{Dist}\left[(\text{lon}_{k_1}^{\text{ATCF}}, \text{lat}_{k_1}^{\text{ATCF}}); (\text{lon}_{k_2}^{\text{ATCF}}, \text{lat}_{k_2}^{\text{ATCF}})\right] \tag{4.23}$$

$$S_{I_k} = D_{I_k} / T_{I_k} \tag{4.24}$$

$$R_{I_k} = \text{Angle}\left[(\text{lon}_{k_1}^{\text{ATCF}}, \text{lat}_{k_1}^{\text{ATCF}}); (\text{lon}_{k_2}^{\text{ATCF}}, \text{lat}_{k_2}^{\text{ATCF}})\right] \tag{4.25}$$

where

- $t_{k_1}^{\text{ATCF}}$ and $t_{k_2}^{\text{ATCF}}$ are the track dates of the first and second bounds of the interval I_k described above,
- $\text{lon}_{k_1}^{\text{ATCF}}$ and $\text{lon}_{k_2}^{\text{ATCF}}$ are the track longitudes of the first and second bound of the interval I_k described above,
- S_{I_k} is the estimated cyclone propagation speed for interval I_k,
- R_{I_k} is the estimated cyclone propagation direction relative to the north for interval I_k.

For each interval I_k, a complex number C_{I_k} is defined as

$$\left|C_{I_k}\right| = S_{I_k} \tag{4.26}$$

$$\arg C_{I_k} = R_{I_k} \tag{4.27}$$

Then, the estimated TC propagation speed and direction are defined as:

$$S_{\text{TC}} = \text{mean}\left[\left|C_{I_1}, ..., C_{I_5}\right|\right] \tag{4.28}$$

$$R_{\text{TC}} = \arg\text{mean}\left[C_{I_1}, ..., C_{I_5}\right] \tag{4.29}$$

where

- S_{TC} is the estimated TC propagation speed,
- R_{TC} is the estimated TC direction angle relative to the north

Rotating the azimuthal equidistant grid

Natively, the SAR swath data grid is defined in a geographical referential. The cyclone propagation direction R_{TC} is used to rotate the data to produce TC oriented data.

Steps to achieve cartesian grid rotation :

1. Create a grid of index (combination of two arrays ranging from 0 to 999)
2. Rotate the index grid (matrix rotation)
3. Because of the rotation, the values of the index grid can now be non-integer. Because we will later use that grid for assignation we need to round them to integer values.
4. Filtering indexes that are out-of-range (higher than 999 or lower than 0)
5. Assign data to a new grid using the rotated grid index, thus achieving the rotation.
6. Rotating variables (`wind_streaks_orientation`, `wind_from_direction`) containing angles by offsetting them by the rotation angle.

A final step is that variables containing angles values have to be shifted to reflect the rotation (`wind_streaks_orientation` and `wind_from_direction`):

- Case where cyclone is in southern hemisphere : $W_{\text{so}} = (-W_{\text{so}} - R_{\text{TC}}) \pmod{360}$
- Case where cyclone is in northern hemisphere : $W_{\text{so}} = (W_{\text{so}} + R_{\text{TC}}) \pmod{360}$

with W_{so} stands for `wind_streaks_orientation` variable.

Converting from azimuthal equidistant grid to polar projection
The cartesian grid, in azimuthal equidistant projection is converted to a polar projection. Instead of `x` and `y` coordinates, describing the data from top left to bottom right, the data is regridded to obtain `rad` and `theta` coordinates. `rad` indicates distance from TC center in meters and `theta` indicates angle from the geographic north in degrees, trigonometrically oriented.

Process parameters used are :

- `pol_rad_reduce`, as described in table 4.1.2.1
- `pol_theta_reduce`, as described in table 4.1.2.1

Input matrix given to polar transformation have a (1000, 1080) shape. They are reduced following the given process parameters. Based on current process parameters values, they are downsampled to a shape of (500, 260). `rad` size is 500 and `theta` size is 360.

Steps to convert from azimuthal equidistant projection to polar projection:

1. Define coordinates arrays, `theta` and `rad`.
2. Convert longitude and latitude arrays to polar using coordinates arrays and a forward transformation.
3. Build a flag array to keep track of valid and invalid data during transformation.
4. Transform the flag array to polar using linearPolar (opencv2 library).
5. Transform data variables to polar using linearPolar.
6. Downsample all data variables following `pol_rad_reduce` and `pol_theta_reduce` parameters values.

Rotating the polar grid
To generate a polar projected grid in TC coordinates, we apply a rotation R_{TC} on the previously constructed polar grid. Rotating in polar projection consists in rotating (or "rolling") the data grids, an operation available in common matrix manipulation libraries (NumPy or Xarray in Python).

As for the rotation of the cartesian grid, variables containing angles values must be shifted to reflect the rotation (`wind_streaks_orientation` and `wind_from_direction` variables):

- Case where cyclone is in southern hemisphere : $W_{\text{so}} = (-W_{\text{so}} - R_{\text{TC}}) \pmod{360}$
- Case where cyclone is in northern hemisphere : $W_{\text{so}} = (W_{\text{so}} + R_{\text{TC}}) \pmod{360}$

with W_{so} as the `wind_streaks_orientation` variable.

4.2.4. TC vortex parameters computation

This section describes TC vortex parameters computation, they are included in the 4 gridded products as described in the product description table 6.2.2.2

TC parameters computation with respect to quadrant are done from the variables defined on polar grids are used for. The computed parameters are :

- `vmax` : maximum wind speed
- `rmax` : radius of the maximum wind speed (`vmax`)
- `r34` : radius where wind speed equals 34 knots
- `r50` : radius where wind speed equals 50 knots
- `r64` : radius where wind speed equals 64 knots

In fact, each parameter is a set of 5 parameters, 1 computed over all quadrants and 1 for each of the four quadrants. In addition, a global `vmax` and `rmax` are computed based on per-quadrants results. The global `vmax` is computed as :

$$\texttt{vmax} = \max(\text{vmax}_{\text{NE}}, \text{vmax}_{\text{SE}}, \text{vmax}_{\text{SW}}, \text{vmax}_{\text{NW}}) \tag{4.30}$$

with NE, SE, SW and NW as the initials of each quadrant.

The global `rmax` is defined as the radius of the global `vmax`.

Furthermore, all parameters, including global ones, are computed both from geographic coordinate grid and TC coordinate grid.

4.2.5. Computing wind components

This section describes wind components calculation. Wind components are added to gridded product, as described in table 6.2.2.2

In all equations presented in this section, the variable `wind_streaks_orientation` (W_{so}) can be replaced by `wind_from_direction` to compute components for that variable.

Meridional, zonal wind components

Meridional and zonal wind components variables are available for products in geographic coordinates. They are computed from `wind_streaks_orientation` and `wind_from_direction` as :

$$Z_{\text{so}} = \cos\left(360 - \text{deg2rad}(W_{\text{so}}) - 90\right) \tag{4.31}$$

$$M_{\text{so}} = \sin\left(360 - \text{deg2rad}(W_{\text{so}}) - 90\right) \tag{4.32}$$

with

- Z_{so} as `zonal_wind_streaks_orientation_component`,
- M_{so} as `meridional_wind_streaks_orientation_component`,
- W_{so} as `wind_streaks_orientation`.

Along track, across track wind components

Along track and across track are similar to meridional and zonal wind components but for for products in TC coordinates. They are computed the same way as meridional and zonal components.

$$A\text{c}_{\text{so}} = \cos\left(360 - \text{deg2rad}(W_{\text{so}}) - 90\right) \tag{4.33}$$

$$A\text{l}_{\text{so}} = \sin\left(360 - \text{deg2rad}(W_{\text{so}}) - 90\right) \tag{4.34}$$

with

- $A\text{c}_{\text{so}}$ as `across_wind_streaks_orientation_component`,
- $A\text{l}_{\text{so}}$ as `along_wind_streaks_orientation_component`,
- W_{so} as `wind_streaks_orientation`.

Polar angle, radial, tangential wind components

Polar angle (θ,`theta`): `theta` variable already exist for polar datasets, as it is defined during conversion from cartesian to polar as described in Section 4.2.3.4. However, `theta` is not defined in cartesian datasets. It is computed as follows:

$$\theta = \left(\arctan 2(y, x) - 90\right) \pmod{360} \tag{4.35}$$

with `y` and `x` as the cartesian coordinates arrays.

Radial, tangential components: Radial and tangential wind components are only defined for grids in TC coordinates, both for polar and cartesian projections. It is defined for `wind_streaks_orientation` and `wind_from_direction` as :

$$R_{\text{so}} = -A\text{c}_{\text{so}} * \cos\text{deg2rad}(\theta) - A\text{l}_{\text{so}} * \sin\text{deg2rad}(\theta) \tag{4.36}$$

$$T_{\text{so}} = -A\text{c}_{\text{so}} * \sin\text{deg2rad}(\theta) + A\text{l}_{\text{so}} * \cos\text{deg2rad}(\theta) \tag{4.37}$$

with

- R_{so} as `radial_wind_streaks_orientation_component`,
- T_{so} as `tangential_wind_streaks_orientation_component`,
- $A\text{c}_{\text{so}}$ as `across_wind_streaks_orientation_component`,
- $A\text{l}_{\text{so}}$ as `along_wind_streaks_orientation_component`

Inflow angle

Inflow angle is defined as :

$$I_{so} = \arctan R_{\text{so}}/T_{\text{so}} \tag{4.38}$$

Parametric inflow angle

5

TCVA Database overview

This chapter provides a general view of the database as well as a few case study examples to illustrate the behavior of the TC center finding algorithm.

5.1. Statistics

About 85% of the from the Level-2 products yield to a Level-3 TCVA. Indeed, few of the acquisitions from the Level-2 database are not over TC center and cannot be used for TC center localization. 57% of the Level-3 TCVA products are flagged as good, yielding to more than 300 highly qualified observations of TC vortex including the TC center and the associated TC parameters (maximum sustained wind speed and wind radii). As obtained, the number of available Level-3 products increased after 2017 when the three C-band SAR (Sentinel-1A, Sentinel-1B and Radarsat-2) were available. Only Radarsat-2 mission is contributing before 2016. Sentinel-1A became a significant contributor in 2016 thanks to SHOC. Since 2022 only Sentinel-1A and Radarsat-2 are contributing to the product because of Sentinel-1B failure. Up to now, the main contributing mission is Sentinel-1 (67%) and in particular Sentinel-1A with 42% of the Level-3 products. Level-3 products allows to sample all TC categories from tropical depression to category-5 over all ocean basins including Atlantic, East Pacific, Central Pacific, West Pacific, Indian ocean and South Hemisphere.

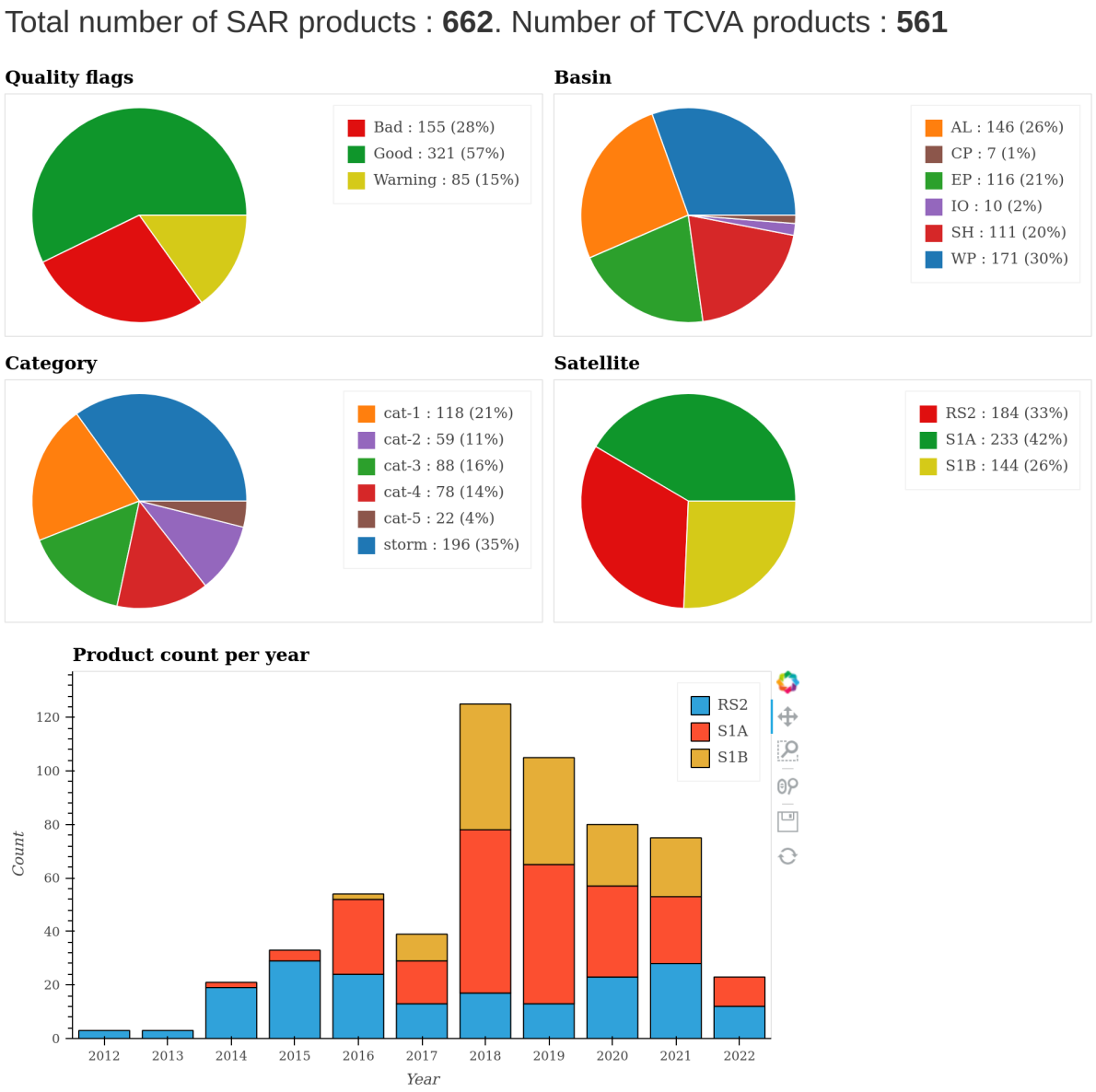

Figure 5.1

As observed on Figure 5.2, the quality of the Level-3 product is less for tropical depression and tropical storm than for higher category hurricanes. This is expected as a well delineated circular and closed eye with sharp eye-wall and strong wind gradient in the outer core is more typical of category-1 and higher intensity storms. For lower intensity storms, beside the possible complex shape of the vortex with an opened and not clear signature for the eye, the radar signal tends to be corrupted by rain which prevents from accurate wind field analysis. Interestingly, when comparing the quality flag (see Figure 5.3) with respect to mission, we note that Radarsat-2 has better performances. This is certainly due to the size of the swath which is larger (450-500km for SCANSAR mode) than for Sentinel-1 (respectively 400 ad 250 km for Extended and Interferometric Wide Swath modes). In contrast, Sentinel-1A and -1B performances are found to be comparable.

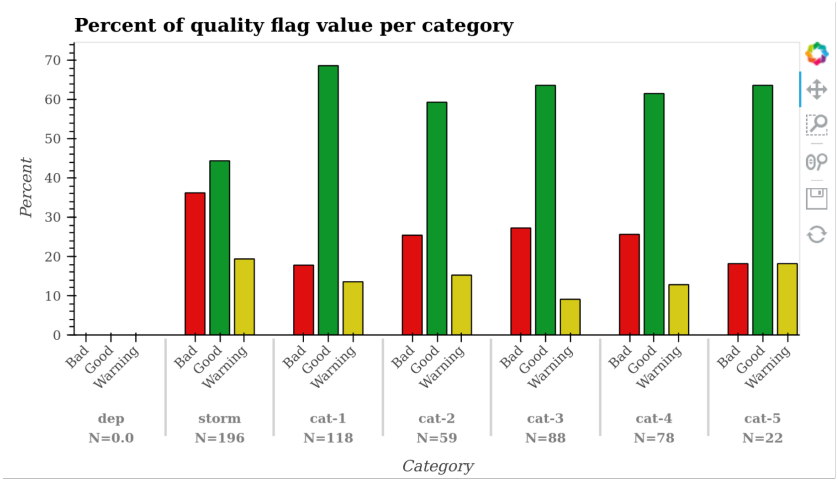

Figure 5.2

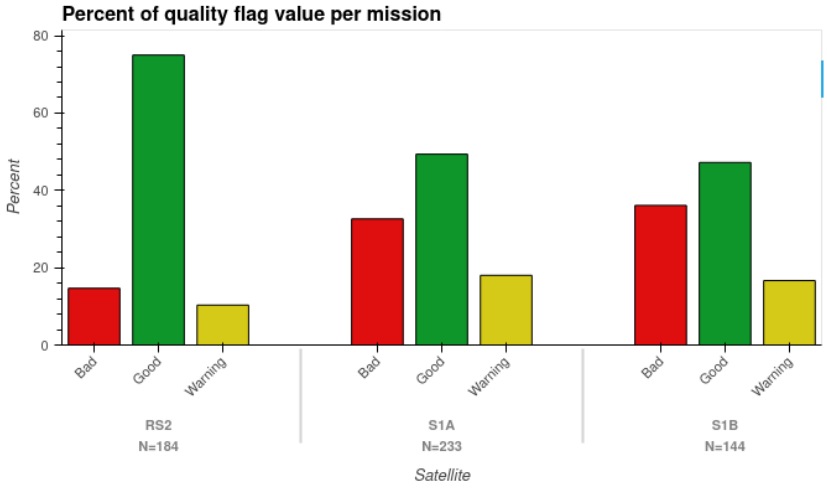

Figure 5.3

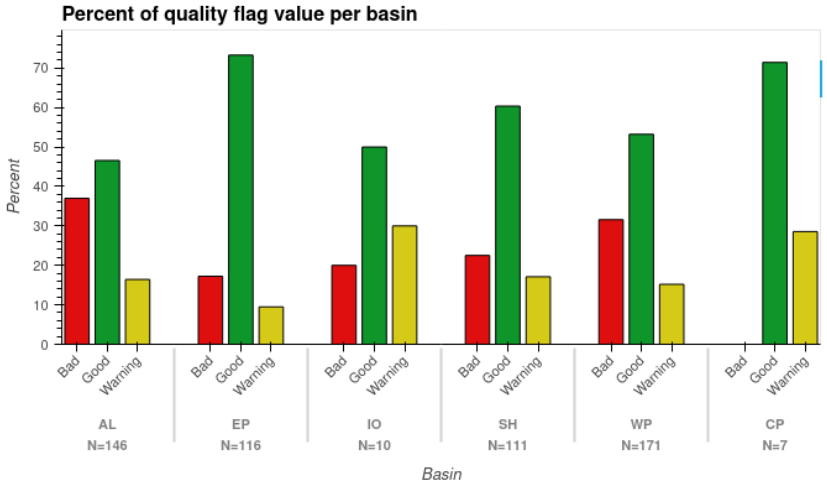

Figure 5.4

In the database, major basins i.e. Atlantic, East Pacific, West Pacific and South Hemisphere are

the most populated with more than 100 Level-3 products for each. A map with the spatial distribution of Level-3 products and associated quality flag is presented on Figure 5.5. As observed most of the unreliable products are located near the coast where the algorithm is known to be less efficient. This is consistent with the analysis for quality flag values performed with respect to basin illustrated on Figure 5.4, which shows that Atlantic and West Pacific have the highest rate of bad quality Level-3 products.

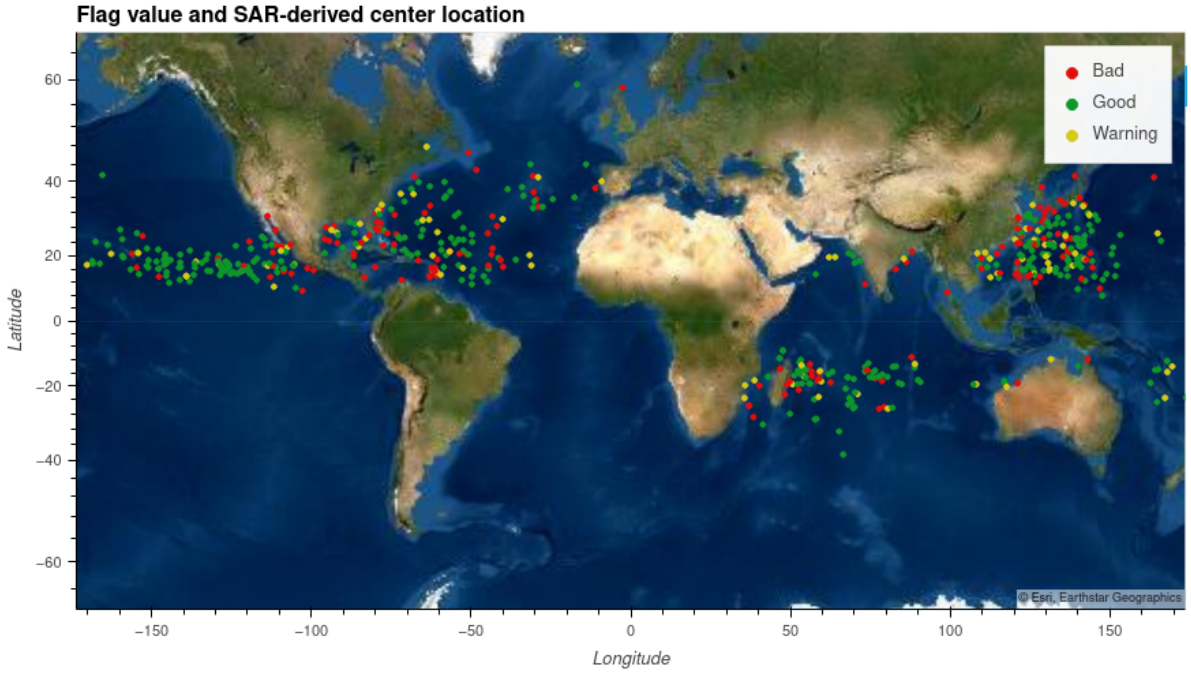

Figure 5.5

5.2. Case study

5.2.1. Case of high intensity cyclone but very small TC eye : PATRICIA - 2015/10/23 - 12:45:50 UTC

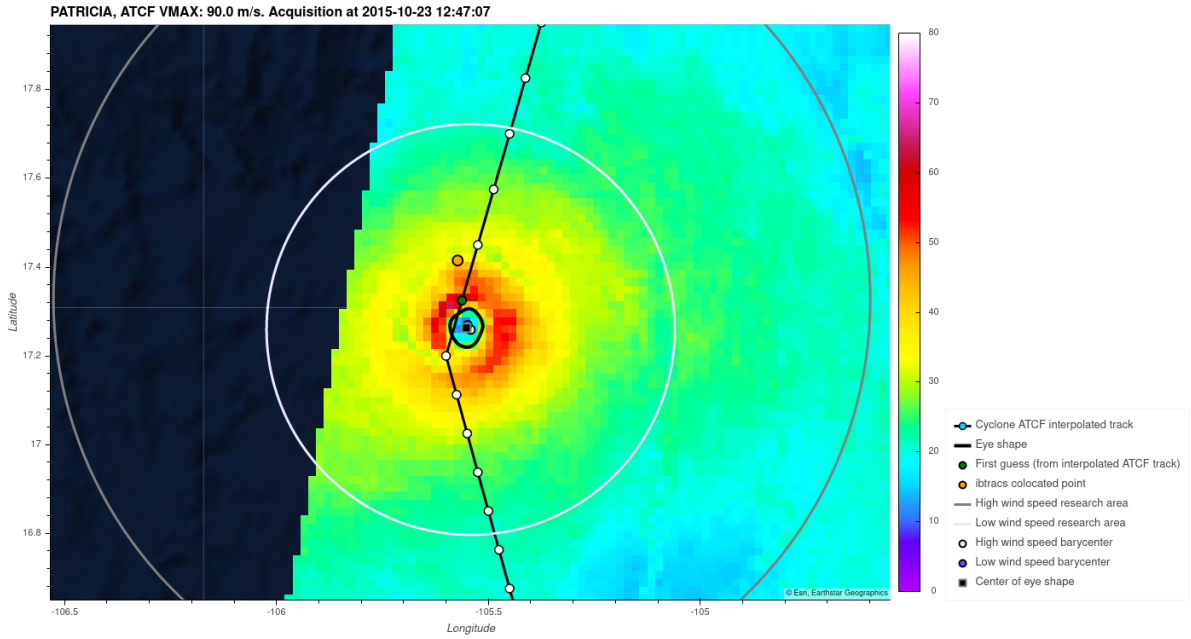

Figure 5.6: SAR acquisition of cyclone PATRICIA, along with TCVA center, eye shape and IBTrACS center.

Flag name	Flag value
center_quality_flag	Warning
track_flag	Bad
lwind_hwind_flag	Good
eye_length_flag	Good
eye_circularity_flag	Good
dist_lwind_flag	Good
eye_contained_flag	Good
distance_center_bbox_flag	Good
distance_track_bbox_flag	Good
land_flag	Good
track_point_flag	Good
percent_eye_bbox_flag	Good

Table 5.1: Flag values for TCVA product on PATRICIA acquisition the 2015-10-23 at 12:45:50

The TCVA algorithm succeeds (see Fig 5.6) on detecting the correct center on TC PATRICIA which is reported category 5 by ATCF at time of acquisition. This is a typical example of a nearly-ideal case for our algorithm, as the cyclone is well-formed (symmetric shape, distinct eye with a clear eye wall).

TC Patricia is characterized by a small eye area and strong wind gradient. SAR high-resolution is able to catch a clear eye wall on this case which allows TCVA to succeed.

The TCVA flags work exactly as they should on this case, excepted for the `track_flag`. The `track_flag` reports bad quality, this could be considered as a false positive, because the TC center is correctly positioned while the error comes from our reference : the IBTrACS point which is mislocated. As the `track_flag` has a strong weight in the calculation of the final product flag `center_quality_flag`, it ends being positioned as warning. We can note that despite the high weight, the aggregated quality flag does not only rely on the `track_flag`, this is beneficial in such cases where IBTrACS is mislocated.

This avoid to wrongly discard data where the TC center location has been successful. This example also suggest that SAR acquisition could be beneficial to produce or validate the IBTrACS TC center.

5.2.2. Case of Eye Replacement Cycle : EMNATI - 2022/02/22 - 02:03:02

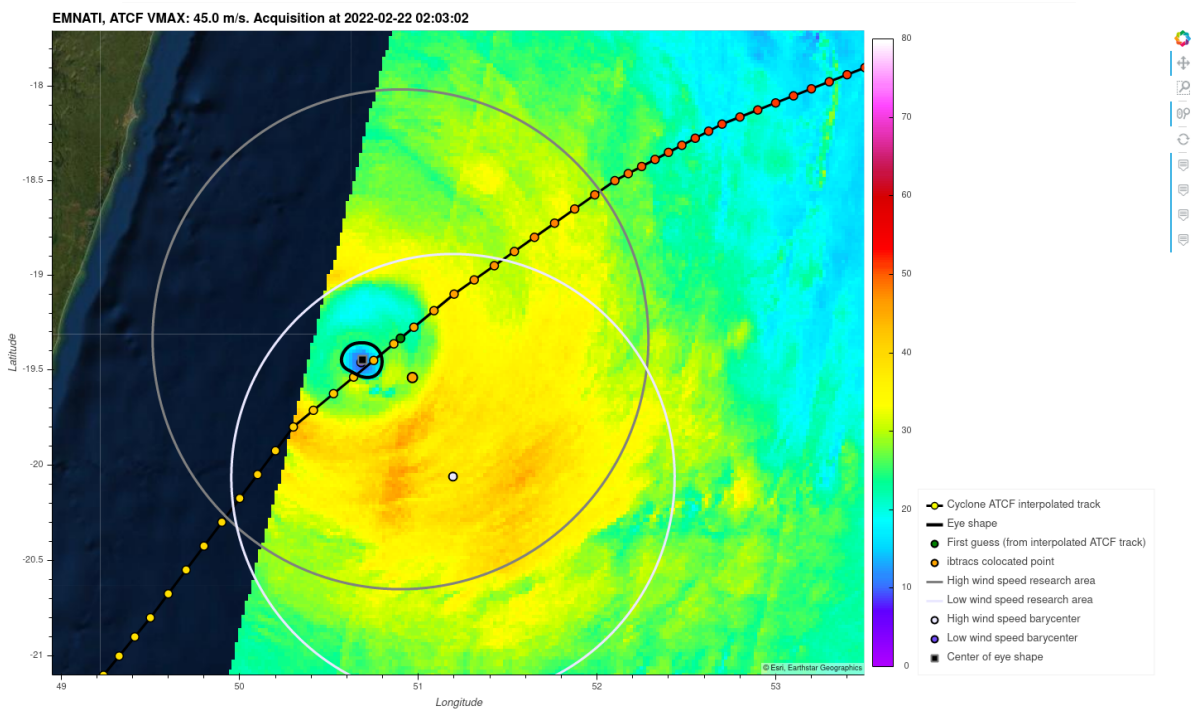

Figure 5.7: SAR acquisition of cyclone EMNATI, along with TCVA center, eye shape and IBTrACS center.

Flag name	Flag value
center_quality_flag	Warning
track_flag	Good
lwind_hwind_flag	Bad
eye_length_flag	Good
eye_circularity_flag	Good
dist_lwind_flag	Good
eye_contained_flag	Good
distance_center_bbox_flag	Good
distance_track_bbox_flag	Good
land_flag	Good
track_point_flag	Good
percent_eye_bbox_flag	Good

Table 5.2: Flag values for TCVA product on EMNATI acquisition the 2022-02-22 at 02:03:02

This example illustrates a less favorable case where the TC undergoes an Eye Replacement Cycle (ERC) while it was reported as a category 2. In such a case, the vortex is characterized by a double eye wall, leading to two rings of strong wind speeds with multiple local minima. In general ERC can confuse the

- RMW estimate : ERC are difficult situation to determine RMW because of the possible confusion between different local maxima of the wind speeds corresponding to different radius. In this case, at the time of acquisition, the ATCF RMW is at 9 km while RMW_CK22 and SAR-derived RMW are larger and close, respectively 45 km and 54 km. From the SAR observation it is likely that

The ATCF RMW was defined with respect to the size of the smallest ring of strong wind speeds, while the two others are comparable to the largest one. In fact, in this case when the acquisition has been performed, it seems that wind speed was stronger in the largest ring of wind speed.

- the localization of the high or low wind speed barycenter : Here the highly off-centered position of the high wind speed barycenter is the consequence of the TC not being fully captured by the satellite image and also because of rain bands that may artificially increase wind speed signal locally. That off-centering could have also resulted in a failure to find the low wind speed area and thus the final TC center. Here this is not the case, the low wind speed barycenter is well located. The TCVA flags correctly inform the user of that potentiality. In this case, the `lwind_hwind_flag` correctly detected the abnormal position of the high wind speed barycenter and is valued to ”Bad” and the `center_quality_flag` is valued to ”Warning” because of the participation of `lwind_hwind_flag` in the weighted sum.
- the eye shape step : This is due to the difficulty for detecting the correct inner eye wall and thus to compute wind gradient. In this case, the wind gradient should have been defined with respect to the second eye-wall (associated with the largest rings corresponding to the strongest wind speed). This is not the case and this yields to a too small eye shape in comparison to the SAR-derived RMW values. It could be expected that the flag responsible for detecting wrong eye shape size (`eye_length_flag`) raises a warning. However it is set to ’good’ because the `eye_length_flag` compares the size of the eye shape to the ATCF RMW value which, in this case, is defined with respect to the size of the smallest eye ring.

5.2.3. Importance of the low wind area : KENNETH 2017-08-19, GONZALO - 2014-10-13, HAGIBIS 2019-10-07

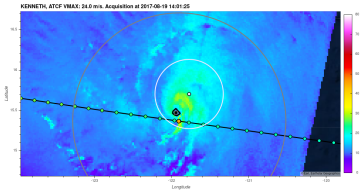

(a) SAR acquisition of cyclone KENNETH, along with TCVA center, eye shape and IBTrACS center. Legend is the same than in Fig. 5.7.

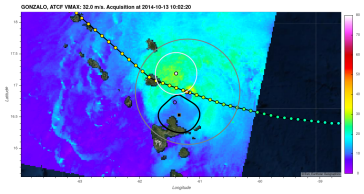

(b) SAR acquisition of cyclone GONZALO, along with TCVA center, eye shape and IBTrACS center. Legend is the same than in Fig. 5.7.

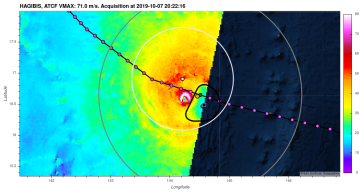

(c) SAR acquisition of cyclone HAGIBIS, along with TCVA center, eye shape and IBTrACS center. Legend is the same than in Fig. 5.7.

Flag name	KENNETH flags	GONZALO flags	HAGIBIS flags
`center_quality_flag`	Good	Bad	Bad
`track_flag`	Good	Bad	Warning
`lwind_hwind_flag`	Warning	Bad	Bad
`eye_length_flag`	Good	Bad	Bad
`eye_circularity_flag`	Good	Good	Good
`dist_lwind_flag`	Good	Bad	Good
`eye_contained_flag`	Good	Good	Bad
`distance_center_bbox_flag`	Good	Good	Bad
`distance_track_bbox_flag`	Good	Good	Bad
`land_flag`	Good	Bad	Good
`track_point_flag`	Good	Good	Good
`percent_eye_bbox_flag`	Good	Good	Bad

Table 5.3: Flag values for TCVA product on KENNETH, GONZALO, HAGIBIS presented acquisitions

This 3 cases are typical difficult cases for the TCVA algorithm. For both GONZALO and HAGIBIS cases, the algorithm fails to find the correct TC center but they are correctly flagged as bad quality. In KENNETH case, the center is correctly found and is correctly flagged as good quality. These 3 cases are characterized by the presence of a low wind speed area outside but near the eye. This makes the

detection of the correct low wind speed area (which should be inside the TC eye) quite challenging. For GONZALO and HAGIBIS the algorithm failed to chose the correct area (see location of the low wind area barycenters on Figure 5.8b and Figure 5.8c.

GONZALO is a case of coastal tropical storm according to ATCF tracks. Land presence and a low maximum wind speed are two factors causing cyclones to deviate from the ideal case for our algorithm as shown in the PATRICIA case in 5.2.1. In practice cases of low maximum wind speeds such as GONZALO and KENNETH often show unclear eye wall, with non-circular eye shapes, a low and distorted gradient between low wind speeds and high wind speeds which makes a correct detection challenging. This results in a higher percentage of bad quality centers for tropical depression and storm, compared to cases above or equal to category 1 TC (as shown in Fig 5.2). GONZALO case triggers several bad flags : `track_flag` and `lwind_hwind_flag` that result from a bad position of the low wind barycenter and thus the final center, `eye_length_flag` and `dist_lwind_flag` indicate issue with the eye shape which is expected because the eye shape does not match the TC eye. Finally, the `land_flag` correctly indicates the presence of land near the TC eye.

HAGIBIS case is more surprising as it is a category 5 TC according to ATCF tracks, with a well-formed eye. However, the presence of a low wind area on the right hand side and in the vicinity of the eye confuses the research of low wind speed area. The small size of the TC eye also contributes to the failure. HAGIBIS also triggers several bad flags : `lwind_hwind_flag` informs here that the low wind speed area is misplaced, `eye_length_flag` correctly tells that the eye shape size is not consistent with the expected TC eye size and `eye_contained_flag`, `distance_center_bbox_flag`, `distance_track_bbox_flag` and `percent_eye_bbox_flag` values are all related to the proximity between the aquisition bounding box border and the computed TC eye.

5.2.4. The eye shape : OMA 2019-02-14, LIONROCK 2016-08-29

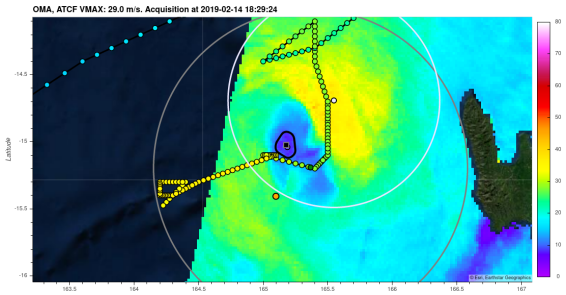

(a) SAR acquisition of cyclone OMA, along with TCVA center, eye shape and IBTrACS center. Legend is the same than in Fig. 5.7.

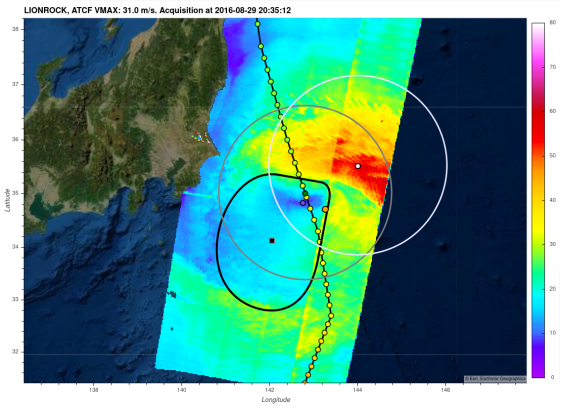

(b) SAR acquisition of cyclone LIONROCK, along with TCVA center, eye shape and IBTrACS center. Legend is the same than in Fig. 5.7.

Flag name	OMA flags	LIONROCK flags
center_quality_flag	Good	Bad
track_flag	Good	Bad
lwind_hwind_flag	Good	Good
eye_length_flag	Bad	Bad
eye_circularity_flag	Good	Good
dist_lwind_flag	Good	Bad
eye_contained_flag	Good	Good
distance_center_bbox_flag	Good	Good
distance_track_bbox_flag	Good	Good
land_flag	Good	Good
track_point_flag	Good	Good
percent_eye_bbox_flag	Good	Good

Table 5.4: Flag values for TCVA product on OMA and LIONROCK presented acquisitions

A particularity of the algorithm is to use the shape of the TC eye from an analysis of the wind gradient in the eye-wall to derive the quality flag of the TC center. In addition, the eye-shape is also included in the product to allow further analysis with respect to this parameter. However, estimating the eye-shape is not always straightforward.

OMA (category 1 TC) and LIONROCK (category 1 TC) cases illustrate typical issues one can get when estimating the eye-shape. An acceptable TC center could be detected for OMA, while the detection on LIONROCK has failed, as shown on Fig 5.9b.

Unlike GONZALO and HAGIBIS previous cases, the discussion is not about failure to find the correct low wind speed area, but a failure to compute a valid eye shape. Indeed, for both OMA and LIONROCK the low wind speed area has correctly been found. However, their eye shape does not look like what is expected. In OMA case, the eye shape is too small, it failed to extend to the the full low wind area. This is because the eye shaping algorithm favour circular shapes, and that it searches for the border with the highest gradient. We can see that OMA's eye content does not have an homogeneous wind speed : it contains a local low wind speed area (lower than the rest of the eye) and a small area of higher wind speed but still inside the eye. For LIONROCK, the issue is that the TC eye does not have a clear eye wall (characterized by a high gradient) on a large portion of the eye (nearly 50%). As a consequence, the eye shape algorithm tries to find a proper eye wall, which turns out to be far from the eye, which result in producing an oversized eye shape.

OMA is considered good quality by the TCVA center quality flag, while a warning flag would be preferred. Whereas LIONROCK is flagged as bad quality. More precisely, it is useful to note that for both cases the `eye_length_flag` indicates bad quality which is expected because we noted that for both cases the area covered by the eye shape is either too big or too small. So, in both cases, `eye_length_flag` successfully reported an issue with the eye shape.

5.2.5. PAULETTE 2020-09-16

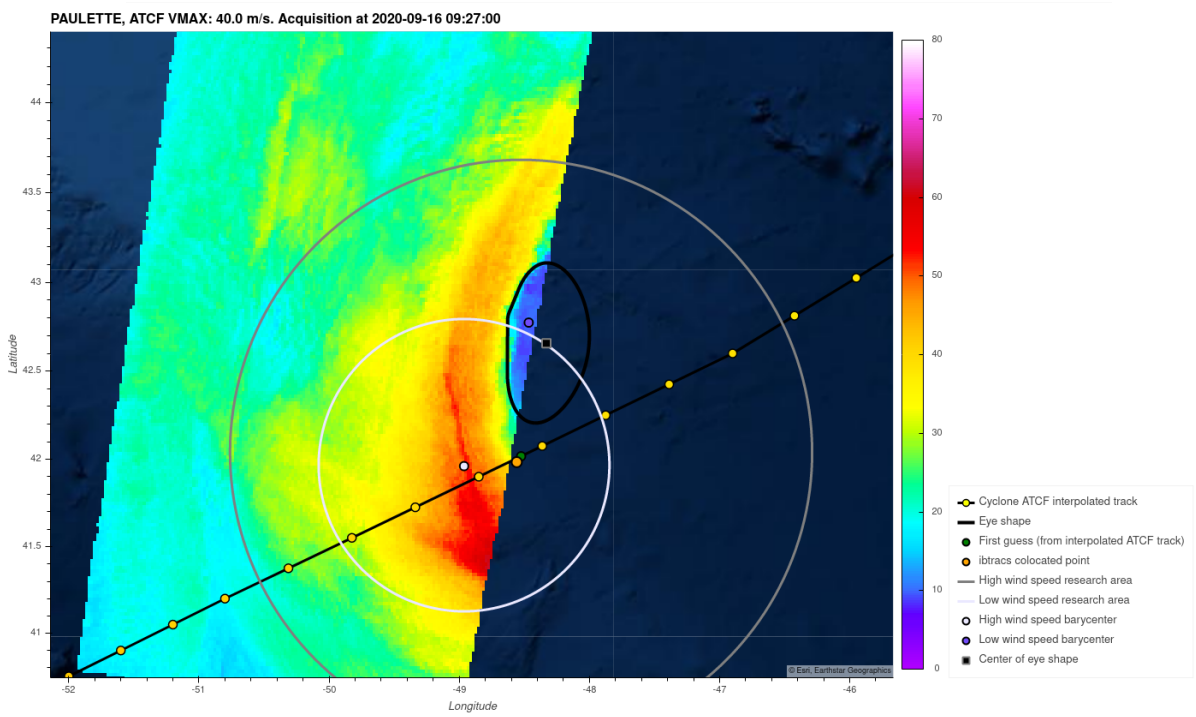

Figure 5.10: SAR acquisition of cyclone PAULETTE, along with TCVA center, eye shape and IBTrACS center.

Flag name	Flag value
center_quality_flag	Bad
track_flag	Bad
lwind_hwind_flag	Bad
eye_length_flag	Warning
eye_circularity_flag	Good
dist_lwind_flag	Good
eye_contained_flag	Bad
distance_center_bbox_flag	Bad
distance_track_bbox_flag	Bad
land_flag	Good
track_point_flag	Bad
percent_eye_bbox_flag	Bad

Table 5.5: Flag values for TCVA product on PAULETTE acquisition the 2020-09-16 at 09:26:22

TCVA center detection failed for presented case TC PAULETTE. Reasons of failure are more straightforward than for previous studied cases and are not inherent to the algorithm. The failure is due to the TC eye being mostly out of the satellite acquisition picture as seen on Fig 5.10. Still the algorithm succeeds in finding a low wind speed area that is probably a part of the TC eye. From that, the eye shape algorithm interpolates to form a closed eye shape, with at least half of it being outside the acquisition. As a consequence, the final center (which is the eye shape barycenter) is placed outside the acquisition.

This case correctly raises nearly all flags to bad or warning quality, except for three, as stated in table 5.5. The `eye_contained_flag` is rarely seen indicating bad quality, because it is switched to bad quality only when the final detected center is outside the acquisition bounding box, which can occur only as a consequence of an important eye shape interpolation.

6

Tropical Cyclone Vortex Analysis product description

This chapter describes the 6 different products of the TCVA product family.

6.1. File naming convention

6.1.1. Gridded products

The base filename structure is the following :

`<satellite>-<acquisition mode>-<algorithm>-<processing flags>-<acquisition start time>-<acquisition stop time>-<resolution in km>-<takeID>_<source sarwing format>_<storm ID>`

Example: `s1b-iw-owi-ca-20211009t104835-20211009t104954-000003-0377A7_sw_wp222021`

Field	Possible values or format
`satellite`	s1a, s1b, rs2
`acquisition mode`	iw, ew
`algorithm`	owi
`processing flags`	cc
`acquisition start time`	YYYYMMDDthhmmss
`acquisition stop time`	YYYYMMDDthhmmss
`resolution in km`	000003 (= 3 km)
`take ID`	6 alphanumeric characters
`source sarwing format`	sw (= swath)
`storm ID`	2 letters for the basin followed by 2 digits for storm number followed by the year.

In addition, a filename suffix is appended to the base filename to discriminate between each of the 4 gridded product to build the complete filename such as:

`<base_filename>_<referential>_<projection>.nc`

Product	File name suffix
Cartesian north-oriented product	`_geogr_gd`
Cartesian cyclone-oriented product	`_cyclone_gd`
Polar north-oriented product	`_geogr_polar`
Polar cyclone-oriented product	`_cyclone_polar`

6.1.2. FIX products description

Per-acquisition FIX file nomenclature mainly uses the source SAR filename. The nomenclature is as follows:

SARFIX_<satellite>-<acquisition mode>-<algorithm>-<processing flags>-<acquisition start time>-<acquisition stop time>-<orbital number>-<take ID>.dat
An example is :
SARFIX_s1a-ew-owi-cc-20190329t140231-20190329t140436-026553-02F9EC.dat

Per-storm acquisition FIX file : SARFIX_b<storm ID>.dat equivalent to SARFIX_b<basin><storm count><year>.dat (ie. SARFIX_bwp252016.dat)

6.2. Gridded products

6.2.1. Gridded products coordinates description

This section describes the coordinates grids of all 4 TC Vortex Analysis netCDF products.

Cartesian grid north-oriented product
This subsection defines the dimensions and grid of the cartesian grid north-oriented product.

Dimensions

- time with a size of 1, indicating timestamp of acquisition
- y with a size of 1000
- x with a size of 1000
- dim_wind_radii with a size of 5, only used for wind radii variables

Grid The x and y arrays define the product grid using an azimuthal equidistant projection. Both x and y ranges from -499 000 meters to 499 000 meters with a step of 1000 meters. The grid center is the computed TC eye center. Each pixel covers an area of 1000x1000 m^2.

Grid orientation The top center of the grid heads to the geographic north.

Cartesian grid cyclone-oriented product
This subsection defines the dimensions and grid of the cartesian grid cyclone-oriented product.

Dimensions

- time with a size of 1, indicating timestamp of acquisition
- y with a size of 1000
- x with a size of 1000
- dim_wind_radii with a size of 5, only used for wind radii variables

Grid The x and y arrays define the product grid using an azimuthal equidistant projection. Both x and y ranges from -499 000 meters to 499 000 meters with a step of 1000 meters. The grid center is the computed TC eye center. Distance between each pixel is 1000 m^2.

Grid orientation The top center of the grid heads towards the cyclone propagation direction

Polar grid north-oriented product
This subsection defines the dimensions and grid of the polar grid north-oriented product.

Dimensions

- time with a size of 1, indicating timestamp of acquisition
- theta with a size of 360
- rad with a size of 500

Grid `theta` and `rad` together define the product a polar grid. `theta` ranges from 0 to 359 degrees with a step of 1 degree, it contains angles in degree relative to the north (0° points to the geographic north), trigonometrically oriented. `rad` ranges from 0 to 499 000 meters with a step of 1000 meters.

Grid orientation `theta` = 0° gives the direction to the geographic north.

Polar grid cyclone-oriented product
This subsection defines the dimensions and grid of the polar grid cyclone-oriented product.

Dimensions

- `time` with a size of 1, indicating timestamp of acquisition
- `theta` with a size of 360
- `rad` with a size of 500

Grid `theta` and `rad` arrays together define the product polar grid. `theta` ranges from 0 to 359 degrees with a step of 1 degree, it contains angles in degree **relative to the cyclone propagation direction** (0° points towards the cyclone propagation direction), trigonometrically oriented. `rad` ranges from 0 to 499 000 meters with a step of 1000 meters

Grid orientation `theta` = 0° gives the direction of the cyclone propagation.

6.2.2. Gridded products variables

Gridded products data variables
This section lists all the data variables available in the 4 gridded products presented in section 3, including their name, unit and a description. Those variables come from the input L2 swath C-Band SAR file, they are regridded to fit on the previously described grids. For more details about them, check the SAR product description. (link to documentation ?)

Variable name	Units	Description
`wind_speed`	m/s	Ocean 10m Wind speed from co- and cross- polarization
`nrcs_cross`	m² / m²	Normalized Radar Cross Section
`nrcs_co`	m² / m²	Normalized Radar Cross Section
`nrcs_detrend_cross`	m² / m²	Nice display
`nrcs_detrend_co`	m² / m²	Nice display
`wind_streaks_orientation`	degrees	Estimation of wind streaks orientation (180° ambiguity) based on local gradient method
`wind_streaks_orientation_stddev`	degrees	Longitude of track steps
`wind_from_direction`	degrees	Wind from direction (meteorologic convention)
`incidence_angle`	degrees	Incidence angle at wind cell center
`heading_angle`	degrees	Platform heading (azimuth from North)
`elevation_angle`	degrees	Elevation Angle at wind cell center
`heterogeneity_mask`	0, 1, 2, 3	Quality flag taking into account the local heterogeneity
`mask_flag`	0, 1, 2, 3	Mask of data (valid, land, ice, no_valid)
`lon`	degrees	Longitude at wind cell center
`lat`	degrees	Latitude at wind cell center

Gridded products analysis variables
This section lists all variables computed during the eye center detection step or during of TC vortex characterization step and available in the 4 gridded products presented in section 3. It includes their name, unit and a description.

Variable name	Units	Description
track_vmax	m/s	ATCF track vmax
cyclone_category		Cyclone category based on track VMAX
eye_shape	lon/lat degrees	Polygon WKT representation of the eye shape.
eye_center	lon/lat degrees	Point WKT representation of the TC eye center.
low_wind_area_barycenter	lon/lat degrees	Point WKT representation of the low wind speed barycenter found by the eye detection algorithm.
high_wind_area_barycenter	lon/lat degrees	Point WKT representation of the high wind speed barycenter found by the eye detection algorithm.
low_wind_research	lon/lat degrees	Polygon WKT representation of the research area within which a stable low wind speed area is researched, to deduce a low wind speed barycenter. Computed by the eye detection algorithm.
high_wind_research	lon/lat degrees	Polygon WKT representation of the research area within which high wind speed pixels are considered to compute a high wind speed barycenter. Computed by the eye detection algorithm.
interpolate_track_point	lon/lat degrees	Point WKT representation of the location of the closest ATCF interpolated track point
track_point_flag	inside, outside	Indicates whether the closest interpolated ATCF track point is inside or outside the satellite acquisition bounding box.
distance_to_coast	meters	Distance of track point to nearest coast. A negative value means track point is inside land.
distance_to_acquisition	meters	Distance of closest interpolated ATCF track point to nearest acquisition border.
percent_outside	percents	Area within 100km around track point outside acquisition bounding box
percent_inside_island	percents	Area of 100km around track point inside acquisition bounding box and on land
percent_non_usable	percents	Sum of percent_outside and percent_inside_island, which is the area of 100km around track point which is unusable for analysis
cyclone_speed	m/s	Estimated cyclone propagation speed
cyclone_speed_std	m/s	Error estimation of cyclone propagation speed
vmax	knots	Maximum sustained wind speed, computed as the max of vmax amongst the 4 quadrants.
rmax	nmi	Radius of the max sustained wind speed (vmax)

Variable name	Units	Description
geo_radii_ms_all	m/s and meters	Computed vmax and radii for all geographically oriented quadrants (NW, NE, SW, SE). 5 values are available : Vmax : maximum wind speed on the wind profile, Rmax : radius of maximum wind speed, R64 : radius where wind speed equals 34 knots, R50 : radius where wind speed equals 50 knots, R34 : radius where wind speed equals 64 knots. -1 means that a correct radius could not be found for that wind speed.
geo_radii_kts_all	knots and nmi	Same as geo_radii_ms_all but units are knots for speeds and nmi for distances.
geo_percent_valid_radii_all	percents	Percent of valid data used for calculation of Vmax, Rmax, R64, R50, R34 for all quadrants for north oriented data.
geo_radii_ms_NE	m/s and meters	Same as geo_radii_ms_all but only for north-east quadrant.
geo_radii_kts_NE	kts and nmi	Same as geo_radii_kts_all but only for north-east quadrant.
geo_percent_valid_radii_NE	percents	Percent of valid data used for calculation of Vmax, Rmax, R64, R50, R34 for north-east quadrant in north oriented data.
geo_radii_ms_SE	m/s and meters	Same as geo_radii_ms_all but only for south-east quadrant.
geo_radii_kts_SE	kts and nmi	Same as geo_radii_kts_all but only for south-east quadrant.
geo_percent_valid_radii_SE	percents	Percent of valid data used for calculation of Vmax, Rmax, R64, R50, R34 for south-east quadrant in north oriented data.
geo_radii_ms_SW	m/s and meters	Same as geo_radii_ms_all but only for south-west quadrant.
geo_radii_kts_SW	kts and nmi	Same as geo_radii_kts_all but only for south-west quadrant.
geo_percent_valid_radii_SW	percents	Percent of valid data used for calculation of Vmax, Rmax, R64, R50, R34 for south-west quadrant in north oriented data.
geo_radii_ms_NW	m/s and meters	Same as geo_radii_ms_all but only for north-west quadrant.
geo_radii_kts_NW	kts and nmi	Same as geo_radii_kts_all but only for north-west quadrant.
geo_percent_valid_radii_NW	percents	Percent of valid data used for calculation of Vmax, Rmax, R64, R50, R34 for north-west quadrant in north oriented data.

Variable name	Units	Description
tco_radii_ms_all	m/s and meters	Computed vmax and radii for all TC oriented quadrants (FR, FL, RR, RL). 5 values are available : Vmax : maximum wind speed on the wind profile, Rmax : radius of maximum wind speed, R64 : radius where wind speed equals 34 knots, R50 : radius where wind speed equals 50 knots, R34 : radius where wind speed equals 64 knots. -1 means that a correct radius could not be found for that wind speed.
tco_radii_kts_all	knots and nmi	Same as tco_radii_ms_all but units are knots for speeds and nmi for distances.
tco_percent_valid_radii_all	percents	Percent of valid data used for calculation of Vmax, Rmax, R64, R50, R34 for all quadrants for TC oriented data.
tco_radii_ms_FR	m/s and meters	Same as tco_radii_ms_all but only for front right quadrant.
tco_radii_kts_FR	kts and nmi	Same as tco_radii_kts_all but only for front right quadrant.
tco_percent_valid_radii_FR	percents	Percent of valid data used for calculation of Vmax, Rmax, R64, R50, R34 for front right quadrant in TC oriented data.
tco_radii_ms_RR	m/s and meters	Same as tco_radii_ms_all but only for rear right quadrant.
tco_radii_kts_RR	kts and nmi	Same as tco_radii_kts_all but only for rear right quadrant.
tco_percent_valid_radii_RR	percents	Percent of valid data used for calculation of Vmax, Rmax, R64, R50, R34 for rear right quadrant in TC oriented data.
tco_radii_ms_RL	m/s and meters	Same as tco_radii_ms_all but only for rear left quadrant.
tco_radii_kts_RL	kts and nmi	Same as tco_radii_kts_all but only for rear left quadrant.
tco_percent_valid_radii_RL	percents	Percent of valid data used for calculation of Vmax, Rmax, R64, R50, R34 for rear left quadrant in TC oriented data.
tco_radii_ms_FL	m/s and meters	Same as tco_radii_ms_all but only for front left quadrant.
tco_radii_kts_FL	kts and nmi	Same as tco_radii_kts_all but only for front left quadrant.
tco_percent_valid_radii_FL	percents	Percent of valid data used for calculation of Vmax, Rmax, R64, R50, R34 for front left quadrant in TC oriented data.

6.2.3. Global attributes

Attribute name	Description
`version`	TC Vortex analysis algorithm version used for product generation
`Storm name`	Official storm name
`Storm ID`	Official storm ID (ie : ep102018)
`Track source file`	ATCF track source filename used as input for first guess (ie : bep102018.dat)
`Source satellite file`	C-Band SAR file used as input

6.3. FIX product description

This section further details the two TC Vortex Analysis FIX products. The difference between per-acquisition and per-storm FIX products lies only in their content, not their structure. Per-storm FIX files simply are concatenation of multiple per-acquisition FIX products.

Our fix format is based on and compatible with the ATCF format decribed in the following link. ATCF FIX formats are csv-like formats, using per-column fields. For convenience, the next paragraph describes the useful columns for this product.

Columns detail

Column number	Column name	Units or format	Description
1	Basin		WP, IO, SH, CP, EP, AL, LS
2	CY		Annual cyclone number, 1-99
3	Date-time	YYYYMMDDHHMM	Fix date-time-group
4	Fix format		Always `70`, meaning analysis
5	Fix type		Measure instrument (S1A, S1B or RS2)
6	Center/intensity	flags	Describes the content of the FIX line. Always `CIR`, meaning for Center fix (lon/lat position) + Intensity fix (max wind speed) + R : wind radii
7	Flagged indicator	flags	Presently empty.
8	Latitude	degrees	Latitude (hundreths of degrees), 0-9000. N/S is the hemispheric index.
9	Longitude	degrees	Longitude (hundreths of degrees), 0-18000. E/W is the hemispheric index.
10	Height of obs	meters	Height of observation, always at `10` for C-Band SAR
11	Posit confidence	flag	Position confidence, `1`: good, `2`: warning, `3`: bad.
12	Wind speed	knots	Maximum sustained wind speed 0-300 kts
13, 14, 15, 16			Presently empty.
17	Radii	knots	Wind intensity radii defined in this record. `34`, `50` or `64`.
18	Radius code		`AAA`: full circle, `NEQ`: northeast quadrant.
19	Rad1	nm	If full circle, radius of specified wind intensity. Otherwise radius of specified wind intensity for northeast quadrant. 0-1200
20	Rad2	nm	Radius of specified wind intensity for southeast quadrant. 0-1200
21	Rad3	nm	Radius of specified wind intensity for southwest quadrant. 0-1200
22	Rad4	nm	Radius of specified wind intensity for northwest quadrant. 0-1200
23, 24, 25, 26, 27			Presently empty.
28	MRD	nm	Radius of maximum winds.
29	Eye diameter	nm	Presently empty.
30	Subregion	flag	`A` - Arabian Sea, `B` - Bay of Bengal, `C` - Central Pacific, `E` - Eastern Pacific, `L` - Atlantic, `P` - South Pacific (135E - 120W), `Q` - South Atlantic, `S` - South IO (20E - 135E), `W` - Western Pacific
31	Fix site		Fix site/WMO Identifier. Always `IFR`
32	Fix enterer		Always `SAR`
33	Analyst initials		Presently empty.
34	Start time	YYYYMMDDHHMM	Fix entry start time
35	End time	YYYYMMDDHHMM	Fix entry end time
36, 37			Presently empty.
38	Observation sources		`RADARSAT-2`, `SENTINEL-1 A` or `SENTINEL-1 B`
39	Comments		Always at `Synthetic Aperture Radar 3KM Wind Speed Analysis`

7

Appendix - TCVA processing flags

During the processing step to find the TC center in each of the Level-2 wind speed product, several flags are also produced to estimate the quality of the different sub-processing steps. A final and global flag is then derived from them to qualify the TC center as derived directly from SAR. The algorithm flowchart of the different processing steps and associated flags is presented on Figure 4.8. This appendix aims at further describing and justifying the thresholds and weights used to define these TC center flags.

7.1. General approach

For each sub-processing step, the associated quality flag can take one of these three possible values :

- 0, meaning good quality,
- 1, meaning warning,
- 2, meaning bad quality.

The global flag `center_quality_flag` is the exception because it aggregates other flag results. While this flag can take continuous values above or equal to 0, meaningful values remain similar to other flags : below 1 the flag indicates good quality, between 1 and 2 it indicates a warning, and above it indicates bad quality.

To define if a flag is either good (0), warning (1) or bad (2), the evaluated criteria (distance, ratio, etc) must be compared to two thresholds, which have to be chosen in order to be meaningful.
The general method for choosing thresholds is the following :

1. Set up a dataset of valid SAR-derived TC centers (human validation).
2. For each evaluated parameter, draw an histogram of the parameter distribution using the previously built dataset.
3. The histogram often looks like a normal distribution. It helps choosing which values must be considered erroneous.
4. Look at cases in the dataset where the currently evaluated parameters looks erroneous based on the histogram.
5. Set up a dataset of invalid SAR-derived TC center (the opposite of the valid dataset).
6. Also draw histograms of the evaluated parameters for invalid dataset, to locate clusters of values that can be used to flag the invalid data, without flagging the valid data.
7. Empirically chose the thresholds, with the help of the histograms. Generally, the ”bad quality” threshold is chosen first, then the ”warning” threshold is chosen relatively to bad quality one.

The `center_quality_flag` summarizes other flag results in one variable, using a weighted sum :

$$\begin{aligned} S_W &= 0.3 \times \text{Eye\_Length\_Flag} + 0.7 \times \text{Track\_Flag} + 0.5 \times \text{Lwind\_Hwind\_Flag} \\ &+ 0.4 \times \text{Dist\_Lwind\_Flag} + 0.9 \times \text{Eye\_Contained\_Flag} \\ &+ 0.25 \times \text{Distance\_Center\_Bbox\_Flag} + 0.25 \times \text{Distance\_Track\_Bbox\_Flag} \\ &+ 0.3 \times \text{Eye\_Circularity\_Flag} + 0.4 \times \text{Track\_Point\_Flag} + 0.9 \times \text{Land\_Flag} \end{aligned}$$

Coefficients of this equation have been chosen to weight each flag with respect to their reliability for estimating the quality of the eye detection algorithm. The reasons for the chosen values are explained in the next sections.

7.2. Track_flag

Track_Flag evaluates the consistency between SAR-derived and IBTrACS TC centers based on the distance between the SAR-derived TC center and the closest interpolated IBTrACs center.

$$D_{\text{RMW}} = \text{Dist}(C_{\text{SAR}}, C_{\text{IBTrACS}})/\text{RMW} \tag{7.1}$$

Threshold

The track_flag threshold for bad quality is set to 1.1 (D_{RMW} >= 1.1 means bad quality). In optimal cases (accurate RMW and accurate IBTrACS TC center location) a D_{RMW} value above 1 means that the found TC center is outside the eye, which means it is incorrect. However, we noted that RMW quality in the IBTrACS is rather poor (as shown in Figure 7.1a).

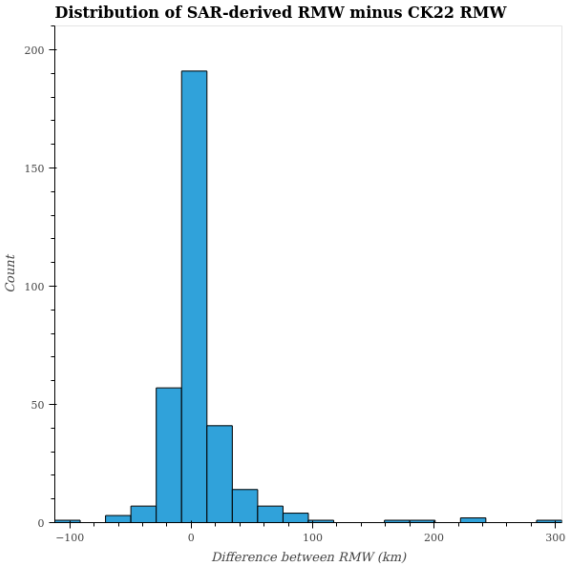

(a) Histogram of difference between RMW computed from reliable TC center (Analysis RMAX is SAR-derived RMAX) and RMW computed using Chavas and Knaff (2022) formula. Analysis RMAX is considered a good reference even if artifacts can be observed.

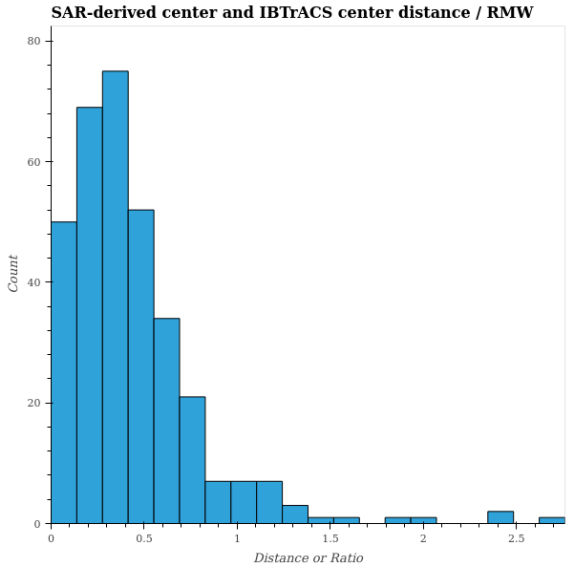

(b) Histogram of distance between the computed TC center and the IBTrACS center for valid SAR-derived TC centers

IBTrACS inaccuracies must thus also be taken into account. A thorough manual analysis of our SAR/IBTrACS dataset leads us to estimate that approximately 8% of the interpolated IBTrACS track TC center locations were undoubtedly wrong (i.e. outside of the TC eye).

To mitigate those inaccuracies and regarding the shape of the Histogram of distance between the computed TC center and the IBTrACS center for valid SAR-derived TC centers as presented on Fig. 7.1b, the track_flag threshold for bad quality has been set to D_{RMW} >= 1.1.

Weight

The track_flag weight contribution to the final center_quality_flag computation is 0.7 to have a heavy weight with respect to other flags (see below). Indeed this flag has a high precision to detect a failed center procedure, mainly because IBTrACS information has proven to be highly reliable when compared to our valid dataset. To note, the weight has not been set to 1 to take into account possible error in the track.

7.3. Lwind_Hwind_flag

The TC center algorithm include several processing steps leading to several intermediate internal variables. Among them, we have:

- High_wind_area_barycenter (C_{LW}): This is the barycenter of the highest wind speed points
- Low_wind_area_barycenter (C_{HW}): This is the barycenter of the lowest wind speed points inside a research radius around the high_wind_area_barycenter (research radius is made so that the low wind speed area falls on the TC eye).

For this flag, D_{LWHW}, the distance between these two intermediate variables, normalized by RMW, is evaluated.

Threshold

The threshold for lwind_hwind_flag bad quality is set to 1.7 (D_{LWHW} >= 1.7)

In optimal cases C_{LW} is close to the true TC center whereas C_{HW} is expected to be close to the true TC center when the area of high wind speed is homogeneous all around the TC eye or close to the location of the maximum wind speed when the high wind area exhibits strong asymmetry. Therefore D_{LWHW} is expected to be about 1.

In fact, as observed in our data, this distance increases with the wind speed area in-homogeneity (e.g. wind speed asymmetry due to the TC translation speed). Rain band can also strongly disturb C_{HW} location and must be taken into account when choosing the threshold (see section for an example). The Figure 7.2 shows the distribution of the distance for D_{LWHW} in the case of valid TC centers. We observe that most values of D_{LWHW} measured for valid TC centers are below 1.5-1.7.

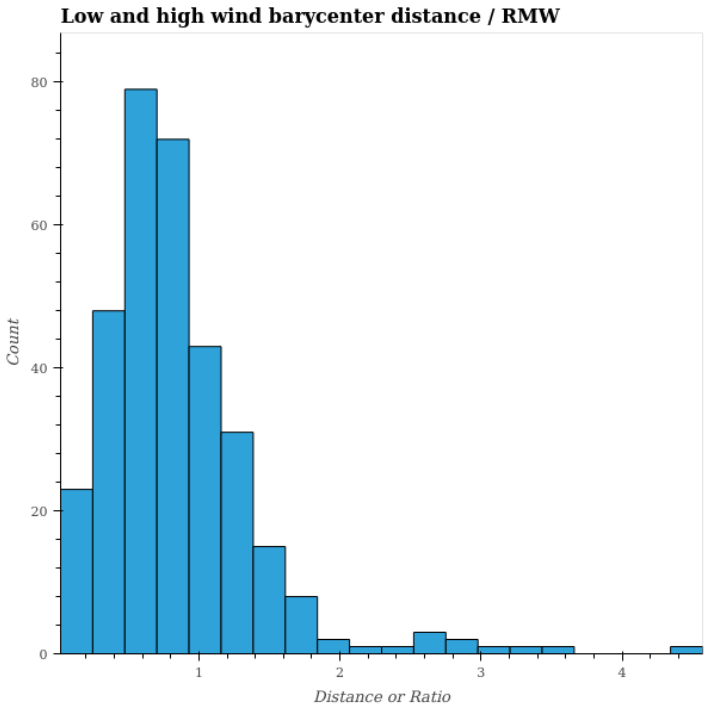

Figure 7.2: Histogram of distance between low wind and high wind barycenters normalized by RMAX CK22, for valid SAR-derived TC centers.

Weight

The lwind_hwind_flag weight contribution to the final center_quality_flag is 0.5.

Figure 7.2 shows that even for valid TC centers, D_{LWHW} can range up to 3.5 for a few cases. Because the high wind speed area barycenter can be strongly impacted by TC wind field asymetry, rain bands or other random phenomenons that can disturb TC ideal shape, this flag cannot be given too much weight. However, it remains a good indicator as Figure 7.2 shows that most valid cases are distributed between 0 and 1.7. The weight of 0.5 has been chosen to be lower than the weight of 0.7 used for track_flag which is considered more stable.

7.4. Eye_length_flag

This flag evaluates the maximum radius of the eye shape.

Threshold

The eye_length_flag threshold for bad quality is set to less than 0.17 or more than 1.2 ($R_{R_{\text{es}},\text{RMW}}$ < 0.17 and $R_{R_{\text{es}},\text{RMW}}$ > 1.2).

In optimal cases, we expect the TC eye shape to be circular and the location of the maximum gradient of wind speed close to the maximum of the wind speed, i.e. to have roughly $R_{R_{\text{es}},\text{RMW}} = 1$.

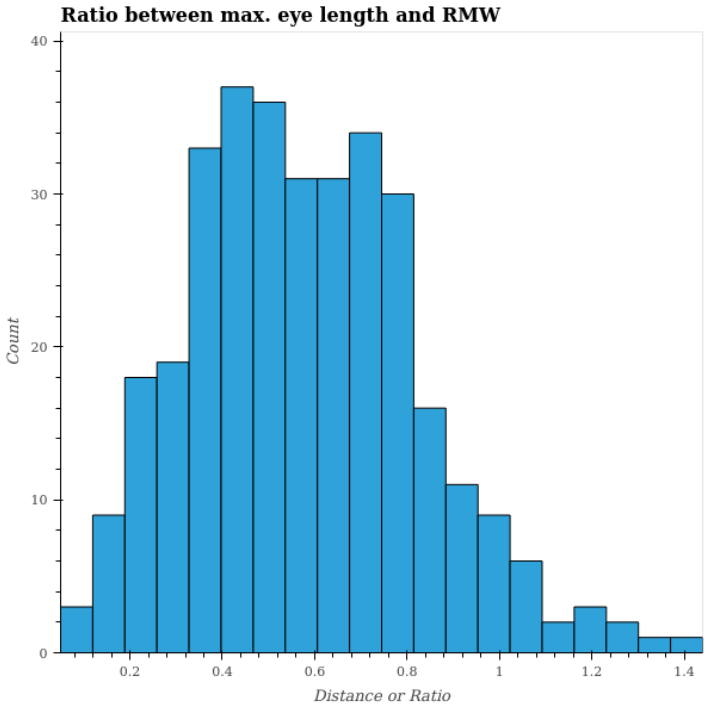

Figure 7.3: Histogram of maximum eyes radius normalized by RMAX CK22, for valid SAR-derived TC centers.

Figure 7.3 shows that most of valid TC centers yield to a $R_{R_{\text{es}},RMW}$ between 0.17 and 1.2. Values higher than 1-1.2 helps detecting erroneous eye shape that are often link to a TC eye without clear gradient on its full circle : On those cases the eye shape is interpolated too far and has a non circular shape (see example at XXXX). Values below 0.17 can indicate an eye shape being calculated on a wrong low wind speed area (outside of the TC eye) or a small local low wind speed area inside the eye. This can occur during TC eye replacement (double eye wall) where several areas associated with a minimum wind speed can be observed.

Weight

The eye_length_flag weight contribution to the final center_quality_flag is set to 0.3. This low weight is justified by the fact that even if the eye shape looks wrong, it does not always result in a wrong TC center but rather in a slightly misplaced one. Thus this flag gives clues to know whether the eye shape algorithm failed and if the TC center location accuracy is may not be optimal.

7.5. Dist_lwind_flag

Dist_Lwind_Flag is obtained by comparing the distance between the low wind speeds area barycenter C_{LW} and the SAR-derived TC center C_{SAR} normalized by the TC RMW.

Threshold

The dist_lwind_flag threshold for bad quality is set to more than 0.8 (D_{LW} > 0.8). In optimal cases, the low wind speeds area barycenter is close to the TC center C_{SAR}. Theoretically a D_{LW} lower than 0.4-0.5

could be expected. But, as observed on our valid TC centers dataset (see Figure 7.4), the analysis of the D_{LW} distribution ranges up to about 0.8.

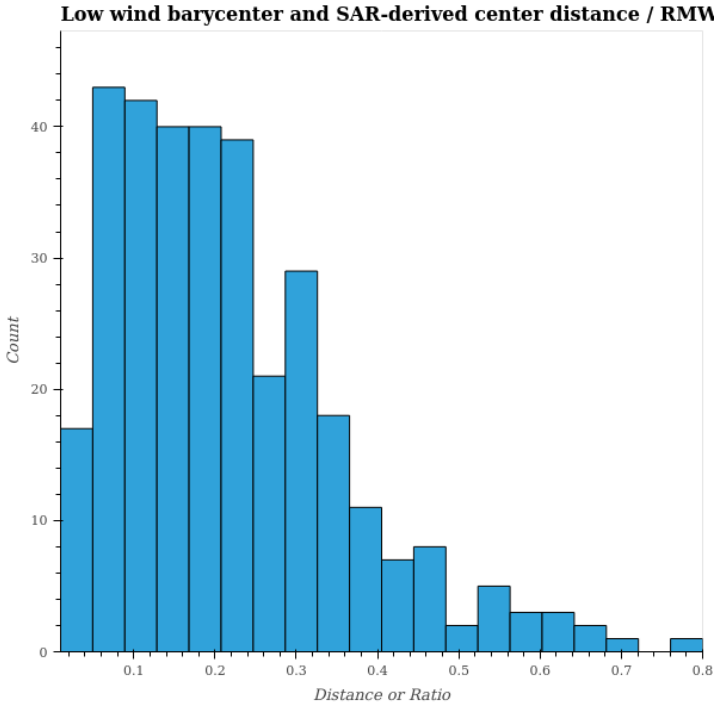

Figure 7.4: Histogram of distance between low wind speeds barycenter and SAR-derived TC center, normalized by RMAX CK22, for valid TC centers.

Weight

The dist_lwind_flag weight contribution to the final center_quality_flag is set to 0.4. As defined, the dist_lwind_flag evaluates the quality of the re-centering post-processing algorithm rather than the TC center finding algorithm. But it can also help detect minor re-centering issues. However it is not best suited for detecting general failure of the TC center algorithm. For example the low wind speeds area barycenter can be wrongly positioned, which will lead to a wrongly positioned center without raising the dist_lwind_flag. Therefore, it can help to detect those general failure cases but it is not sufficient in itself and must be associated with other flag for a complete diagnosis.

7.6. Eye_circularity_flag

Threshold

The eye_circularity_flag threshold is set to 0.65 so that T_{eye} < 0.65 means that centering may suffer from issues, leading to low values of eye shape thinness ratio. Indeed, for well-formed cyclones, we expect T_{eye} to be close to 1. As osbserved on Figure 7.5a, the distribution of T_{eye} indicates that for valid SAR-derived TC centers T_{eye} can go as low as 0.74.

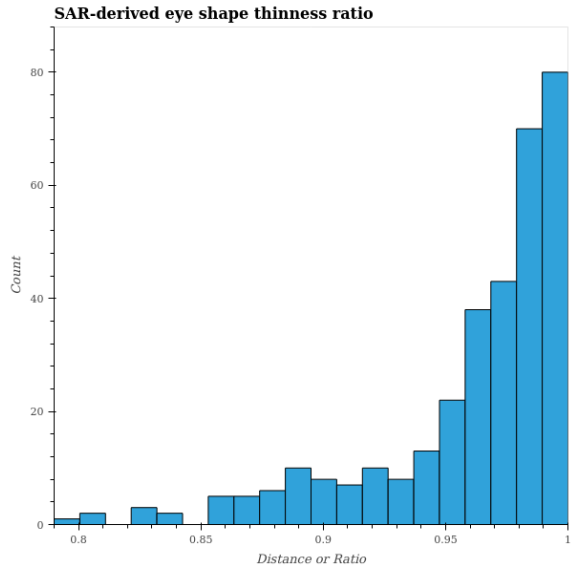

(a) Histogram of eye shape thinness ratio T_{eye}, for valid SAR-derived TC centers.

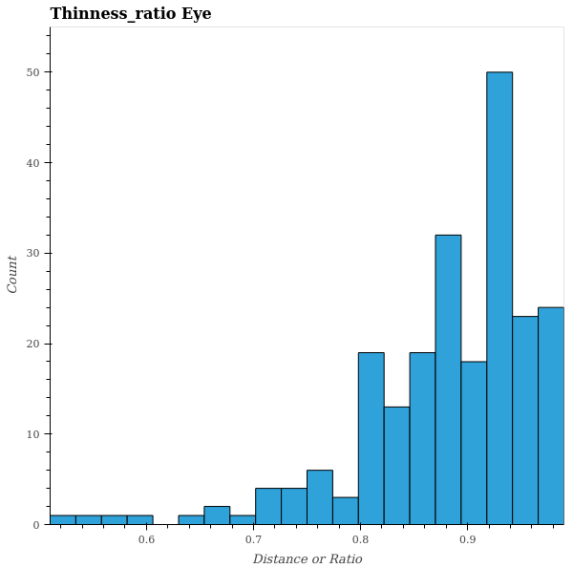

(b) Histogram of eye shape thinness ratio T_{eye}, for invalid SAR-derived TC centers.

However, Figure 7.5b shows that for the invalid dataset, there is a cluster of high counts between 0.6 and 0.7. After manual inspection on some of these cases, we concluded that cases having T_{eye} between 0.65 and 0.75 needed a warning value for the eye_circularity_flag, because some of these eye shape were nearly right while still having a non-circular shape (due to erratic nature of the corresponding TC eye).

Weight

The eye_circularity_flag weight contribution to the final center_quality_flag is 0.3. This low weight is justified by the fact that even if the eye shape looks wrong, it does not always result in a totally wrong center but rather in a slightly misplaced one. It gives clues to know if the eye shape algorithm failed and thus if the center precision is degraded.Even if this flag helps detecting center detection failure, the final flag cannot rely too much on it (as it focuses on the eye shape quality) and the diagnosis must be completed using other flags.

7.7. Distance_center_bbox_flag

This section also applies to the the distance_track_bbox_flag.

7.7.1. Threshold

The distance_center_bbox_flag threshold is set to 25000 so that $D_{C_{\text{SAR}},\text{BBB}}$ < 25000 means bad quality This threshold value has been chosen more arbitrarily than the others. However, the motivation behind this value is that TC in cat-1 or higher has typically a radius of maxium wind speed lower than 40 km. This means that if $D_{C_{\text{SAR}},\text{BBB}}$ is lower than 25000, then there is high chances that the eye has not be fully captured by the SAR acquisition, the center being located to close to the swath.

Weight

The distance_center_bbox_flag weight contribution to the final center_quality_flag is 0.25. This flag weight can be combined with the distance_track_bbox_flag which relies on the same principle and the same weight of 0.25.

7.8. Land_flag

Threshold

The land_flag threshold for bad quality is set to 3%, so that P_{Land} > 3, means bad quality.

The threshold has arbitrarily been set to 3% to detect if there is significant presence of land. Indeed, this often disturb the development of a canonical vortex, possibly leading to less accurate eye center detection.

Weight
The land_flag weight contribution to the final center_quality_flag is 0.9. This high weight is justified by the fact that when land appears on the image, portion of data are truncated, where no wind speed can be estimated. This also can also creates artefact in the wind speed measurement near the coast (because of inaccurate land mask in the Level-2 wind product), creating outliers which can impact the TC center retrieval.

7.9. Percent_eye_bbox_flag

Threshold
The percent_eye_bbox_flag threshold for bad quality is set to 70% so that a case with $P_{\text{Eye,BBB}} \leq 70\%$ is considered as bad quality.

The threshold has been chosen arbitrarily, by looking at specific cases (see example at section XXXXXXXX) which had eye near the acquisition border but with eye shape correctly interpolated. The main percent_eye_bbox_flag goal is to re-qualify distance_center_bbox_flag and distance_track_bbox_flag to lower their value especially when the eye is near the acquisition edge but that percent_eye_bbox_flag informs that the eye shape has not been interpolated too much outside of the acquisition and that the re-center procedure has chances to have succeeded.

Weight
Percent_eye_bbox_flag is directly not included in the computation of the center_quality_flag.

Bibliography

Banal, S., Iris, S., and Saint-Jean, R. (2007). Canadian Space Agency; Hurricane Watch Program: Archive contents, Data Access and improved planning strategies. In *2007 IEEE International Geoscience and Remote Sensing Symposium*, pages 3494–3497. IEEE.

Chavas, D. R. and Knaff, J. A. (2022). A simple model for predicting the tropical cyclone radius of maximum wind from outer size. *Weather and Forecasting*, 37(5):563–579.

Combot, C., Mouche, A., Knaff, J., Zhao, Y., Zhao, Y., Vinour, L., Quilfen, Y., and Chapron, B. (2020). Extensive high-resolution synthetic aperture radar (sar) data analysis of tropical cyclones: Comparisons with sfmr flights and best track. *Monthly Weather Review*, 148(11):4545 – 4563.

Holland, G. J., Belanger, J. I., and Fritz, A. (2010). A revised model for radial profiles of hurricane winds. *Monthly Weather Review*, 138(12):4393 – 4401.

Horstmann, J., Falchetti, S., Wackerman, C., Maresca, S., Caruso, M. J., and Graber, H. C. (2015). Tropical Cyclone Winds Retrieved From C-Band Cross-Polarized Synthetic Aperture Radar. *IEEE Transactions on Geoscience and Remote Sensing*, 53(5):2887–2898.

Horstmann, J., Wackerman, C., Falchetti, S., and Maresca, S. (2013). Tropical Cyclone Winds Retrieved From Synthetic Aperture Radar. *Oceanography*, 26(2).

Jackson, C. R., Ruff, T. W., Knaff, J. A., Mouche, A., and Sampson, C. R. (2021). Chasing cyclones from space. *Eos*, 102.

Katsaros, K., Vachon, P. W., Black, P., Dodge, P., and Uhlhorn, E. (2000). Wind Fields from SAR: Could They Improve Our Understanding of Storm Dynamics? Technical report.

Mouche, A., Chapron, B., Knaff, J., Zhao, Y., Zhang, B., and Combot, C. (2019). Copolarized and Cross□Polarized SAR Measurements for High□Resolution Description of Major Hurricane Wind Structures: Application to Irma Category 5 Hurricane. *Journal of Geophysical Research: Oceans*, 124(6):3905–3922.

Mouche, A. A., Chapron, B., Zhang, B., and Husson, R. (2017). Combined Co- and Cross-Polarized SAR Measurements Under Extreme Wind Conditions. *IEEE Transactions on Geoscience and Remote Sensing*, 55(12):6746–6755.

Reul, N., Chapron, B., Zabolotskikh, E., Donlon, C., Mouche, A., Tenerelli, J., Collard, F., Piolle, J. F., Fore, A., Yueh, S., Cotton, J., Francis, P., Quilfen, Y., and Kudryavtsev, V. (2017). A New Generation of Tropical Cyclone Size Measurements from Space. *Bulletin of the American Meteorological Society*, 98(11):2367–2385.

Sampson, C. R. and Schrader, A. J. (2000). The Automated Tropical Cyclone Forecasting System (Version 3.2). *Bulletin of the American Meteorological Society*, 81(6):1231–1240.

Vinour, L., Jullien, S., Mouche, A., Combot, C., and Mangeas, M. (2021). Observations of tropical cyclone inner-core fine-scale structure, and its link to intensity variations. *Journal of the Atmospheric Sciences*, 78(11):3651–3671.

Zhang, B. and Perrie, W. (2012). Cross-Polarized Synthetic Aperture Radar: A New Potential Measurement Technique for Hurricanes. *Bulletin of the American Meteorological Society*, 93(4):531–541.

Zheng, G., Yang, J., Liu, A. K., Li, X., Pichel, W. G., He, S., and Yu, S. (2017). Observing typhoons from satellite-derived images. In *Hurricane Monitoring With Spaceborne Synthetic Aperture Radar*, pages 183–214. Springer.